



การศึกษาเคมีแสงและเคมีความร้อนของสารประกอบอินทรีย์และสารประกอบเชิงซ้อนชนิดใหม่ใน
การเกิดปฏิกิริยากับโปรตีน

STUDY OF PHOTOCHEMISTRY AND THERMAL CHEMISTRY OF NEWLY DESIGNED
ORGANIC COMPOUNDS AND A METAL COMPLEX TOWARDS INTERACTIONS WITH
PROTEINS

BENCHAWAN JITYUTI

Graduate School Srinakharinwirot University

2019

การศึกษาเคมีแสงและเคมีความร้อนของสารประกอบอินทรีย์และสารประกอบเชิงซ้อน
ชนิดใหม่ในการเกิดปฏิกิริยากับโปรตีน



ปริญญานิพนธ์นี้เป็นส่วนหนึ่งของการศึกษาตามหลักสูตร
ปรัชญาดุษฎีบัณฑิต สาขาวิชาเคมีประยุกต์
คณะวิทยาศาสตร์ มหาวิทยาลัยศรีนครินทรวิโรฒ
ปีการศึกษา 2562
ลิขสิทธิ์ของมหาวิทยาลัยศรีนครินทรวิโรฒ

STUDY OF PHOTOCHEMISTRY AND THERMAL CHEMISTRY OF NEWLY
DESIGNED ORGANIC COMPOUNDS AND A METAL COMPLEX TOWARDS
INTERACTIONS WITH PROTEINS



BENCHAWAN JITYUTI

A Dissertation Submitted in partial Fulfillment of Requirements
for DOCTOR OF PHILOSOPHY (Applied Chemistry)
Faculty of Science Srinakharinwirot University

2019

Copyright of Srinakharinwirot University

THE DISSERTATION TITLED

STUDY OF PHOTOCHEMISTRY AND THERMAL CHEMISTRY OF NEWLY DESIGNED
ORGANIC COMPOUNDS AND A METAL COMPLEX TOWARDS INTERACTIONS WITH
PROTEINS

BY

BENCHAWAN JITYUTI

HAS BEEN APPROVED BY THE GRADUATE SCHOOL IN PARTIAL FULFILLMENT OF THE
REQUIREMENTS FOR THE DOCTOR OF PHILOSOPHY IN APPLIED CHEMISTRY
AT SRINAKHARINWIROT UNIVERSITY

Dean of Graduate School

(Assoc. Prof. Dr. Chatchai Ekpanyaskul, MD.)

ORAL DEFENSE COMMITTEE

..... Major-advisor Chair
(Assoc. Prof. Dr. Apinya Chaivisuthangkura) (Asst. Prof. Dr. Patchareenart Saparpakorn)

..... Co-advisor Committee
(Assoc. Prof. Dr. Teerayuth Liwporncharoenvong) (Assoc. Prof. Dr. Siritron Samosorn)

..... Co-advisor
(Dr. Pornthip Boonsri)

Title	STUDY OF PHOTOCHEMISTRY AND THERMAL CHEMISTRY OF NEWLY DESIGNED ORGANIC COMPOUNDS AND A METAL COMPLEX TOWARDS INTERACTIONS WITH PROTEINS
Author	BENCHAWAN JITYUTI
Degree	DOCTOR OF PHILOSOPHY
Academic Year	2019
Thesis Advisor	Associate Professor Dr. Apinya Chaivisuthangkura

In this study, the ability of new chemical reagents, a pyrene derivative, fluorescein derivatives, and a metal complex, to initiate the cleavage of proteins at specific sites was investigated. The selective cleavage of bovine serum albumin (BSA) by PMA-IB was successful by irradiating the mixture of BSA and PMA-IB at 346 nm, in the presence of electron acceptor, cobalt (III) hexamine trichloride (CoHA). The cleavage of BSA resulted in two new fragments with molecular weights of approximately 45 and 22 kDa. The spectroscopic method and molecular docking indicated that PMA-IB was bound to BSA with a high binding affinity and the location of PMA-IB was located within the subdomain IIIB of BSA. Fluorescein sodium salt (F-1), 5(6)-carboxyfluorescein diacetate (F-2) and biotin-4-Fluorescein (F-3) were also selected as fluorescent probes for initiation of the protein cleavage reaction. All three probes cleaved lysozyme and avidin after exposure the light at 490 - 494 nm, in the presence of CoHA. N-terminal amino acid sequencing of peptide fragments indicated the cleavage site of lysozyme between Trp108 and Val109 for all three probes, while the cleavage of avidin by F-1 and F-2 was detected between Trp70 – Lys71. However, the cleavage site of avidin by F-3 could not be determined due to small cleavage yields. In addition, the spectroscopic method and molecular docking studies clarified the binding location and binding affinity of F-1, F-2 and F-3 on lysozyme and avidin, corresponding with the results obtained from the protein photocleavage experiments. In case of metal complex, $\text{MoO}(\text{O}_2)_2(\text{asparagine})(\text{H}_2\text{O})$ successfully cleaved pepsin by activating it with light (320 and 340 nm) and heat (37 °C), without the requirement of a reducing agent and H_2O_2 . The cleavage of pepsin resulted in at least two fragments with molecular weights of 22 and 9 kDa in photoreaction, and resulted in at least three fragments with molecular weights of 30, 26 and 22 kDa for a thermal reaction. These synthesized chemical reagents can serve as potential artificial peptidases for applications in biological fields, and can be applied in the design of novel therapeutic agents in the future.

Keyword : Photochemistry, Thermal Chemistry, Newly Designed Organic Compounds, Metal Complex

ACKNOWLEDGEMENTS

This dissertation can be successful because I received advice, help and support from many people. First of all, I am very grateful to my advisor, Associate Professor Dr. Apinya Chaivisuthangkura for her assistance and suggestions during the planning and development of this research work. This dissertation would be impossible without her support. I am also very grateful to my co-advisors, Associate Professor Dr. Teerayuth Liwporcharoenwong and Dr. Pornthip Boonsri for their help and guidance. Their suggestions helped me anytime during my thesis.

I would like to thank the oral defense committee, Assistant Professor Dr. Patchreenart Saparpakorn and Associate Professor Dr. Siritron Samosorn for their kindness and valuable comments to improve my thesis.

I would like to thank the financial supports provided by the Thailand Research Fund (The Royal Golden Jubilee Ph.D. program).

I would like to express my sincere to Professor Dr. Koichi Kato and his team for their suggestions and supervision throughout the period time in his laboratory at the Institute for Molecular Science and Okazaki Institute for Integrative Bioscience, Okazaki, Japan.

I am grateful to Assistant Professor Dr. Mayuso Kuno for his advice and help me in this research work. I would like to thank the kindness of Dr. Arthit Makarasen at Chulabhorn Research Institute for his suggestions and allowing me to use the facilities in his laboratory.

I would like to thank Department of Chemistry, Faculty of Science, Srinakharinwirot University for providing equipment and instruments on my thesis.

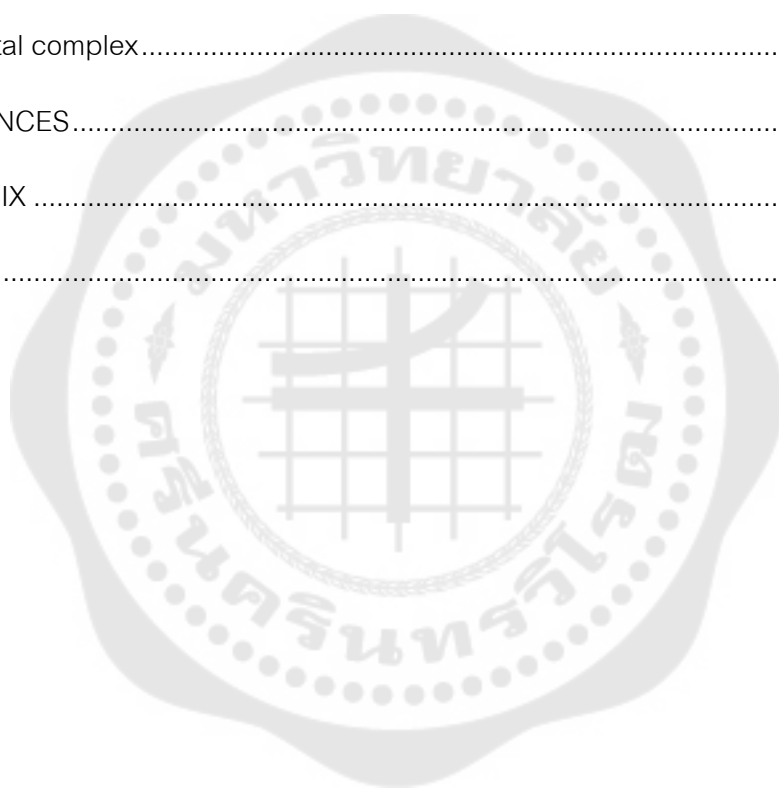
Finally, I am deeply grateful to my family for all their support throughout the duration of this research work and general life.

BENCHAWAN JITYUTI

TABLE OF CONTENTS

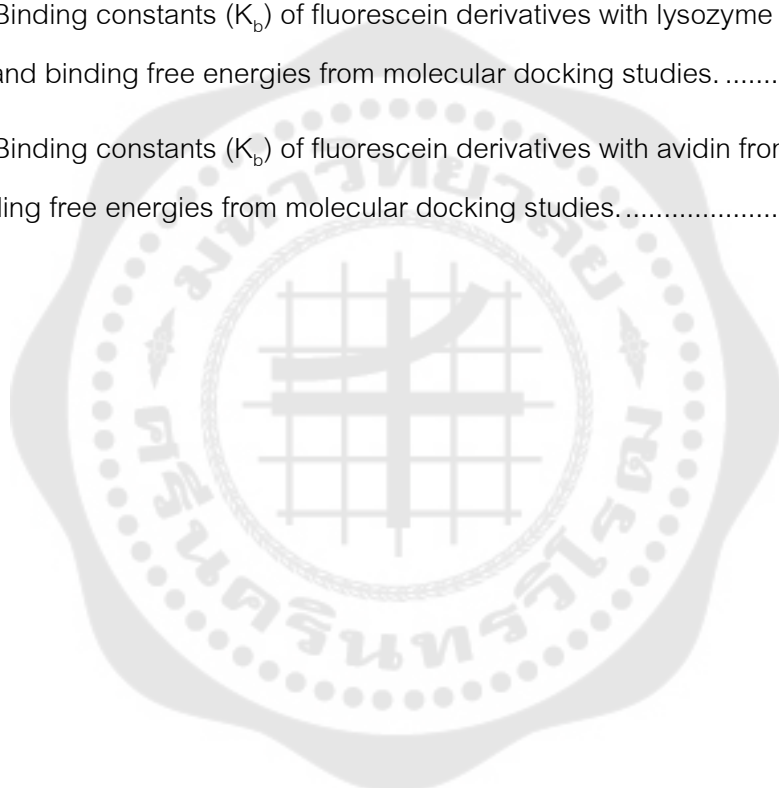
	Page
ABSTRACT	D
ACKNOWLEDGEMENTS.....	E
TABLE OF CONTENTS.....	G
LIST OF TABLES.....	I
LIST OF FIGURES	J
CHAPTER 1 INTRODUCTION	1
Background.....	1
Objectives of the study	3
Significance of the study.....	3
Scope of the study	3
CHAPTER 2 REVIEW OF THE LITERATURE.....	5
1. Proteins	5
2. Cleavage of protein.....	6
3. Spectroscopic methods.....	8
4. Molecular docking	10
5. Related research.....	10
CHAPTER 3 METHODOLOGY	20
1. Equipment	20
2. Chemical reagents	20
3. Methods	22
CHAPTER 4 FINDINGS	28

1. Pyrene derivative.....	29
2. Fluorescein derivatives	36
3. Metal complex.....	60
CHAPTER 5 CONCLUSION AND DISCUSSION.....	67
1. Pyrene derivative.....	67
2. Fluorescein derivatives	68
3. Metal complex.....	69
REFERENCES.....	71
APPENDIX	76
VITA	83



LIST OF TABLES

	Page
Table 1 Binding properties of fluorescein derivatives with lysozyme.....	45
Table 2 Binding properties of fluorescein derivatives with avidin.	47
Table 3 The quenching constants (K_{SV}) of fluorescein derivatives with CoHA.	49
Table 4 Binding constants (K_b) of fluorescein derivatives with lysozyme from binding studies and binding free energies from molecular docking studies.	55
Table 5 Binding constants (K_b) of fluorescein derivatives with avidin from binding studies and binding free energies from molecular docking studies.....	59



LIST OF FIGURES

	Page
Figure 1 Basic structure of amino acid.	5
Figure 2 Formation of a peptide bond.	6
Figure 3 Structure of sodium dodecyl sulfate (SDS).	7
Figure 4 Structure of Py-Phe.	11
Figure 5 Binding properties of the probe on protein (a) lysozyme and (b) BSA.....	12
Figure 6 Structures of the Py-Phe analogs.	12
Figure 7 Structures of pyrenyl peptides: Py-Gly-X, where X = phenylalanine (Py-Gly-Phe), tyrosine (Py-Gly-Tyr), tryptophan (Py-Gly-Trp), and histidine (Py-Gly-His).	13
Figure 8 Structure of Py-biotin.....	14
Figure 9 Structure of ibuprofen.	14
Figure 10 Crystal structure of HAS.....	15
Figure 11 Structures of (a) biotin-4-fluorescein and (b) biotin-4-FITC.	16
Figure 12 Structure of fluorescein sodium salt.	16
Figure 13 Structure of fluorescein.	17
Figure 14 General procedure for cleavage of protein by metal complexes.	18
Figure 15 Structures of Co (III) complexes.	18
Figure 16 Structure of $\text{MoO}(\text{O}_2)_2(\alpha\text{-leucine})(\text{H}_2\text{O})$	19
Figure 17 (a) Preparation of gel sandwiched and (b) Mini Trans-Blot [®] Electrophoretic Transfer Cell.	26
Figure 18 Structure of PMA-IB.	29
Figure 19 Absorption spectrum of PMA-IB (10 μM).	29

Figure 20 SDS-PAGE of the cleavage reaction of BSA with PMA-IB.	30
Figure 21 SDS-PAGE of the cleavage reaction of HSA with PMA-IB.	31
Figure 22 Absorption spectra of PMA-IB in the absence and presence of BSA.	32
Figure 23 The Stern-Volmer quenching plot of PMA-IB by CoHA in the absence and presence of BSA.	33
Figure 24 The structure of PMA-IB docked in BSA.	34
Figure 25 Structures of fluorescein derivatives: (a) Fluorescein sodium salt (F-1), (b) 5(6)-Carboxyfluorescein diacetate (F-2) and (c) Biotin-4-Fluorescein (F-3).	36
Figure 26 SDS-PAGE of lysozyme from the cleavage reaction with F-1.	37
Figure 27 SDS-PAGE of lysozyme from the cleavage reaction with F-2.	38
Figure 28 SDS-PAGE of lysozyme from the cleavage reaction with F-3.	38
Figure 29 SDS-PAGE of lysozyme from the cleavage reaction with fluorescein derivatives.	39
Figure 30 The cleavage yields of peptide fragments from the photoreaction of lysozyme with three fluorescein derivatives.	40
Figure 31 SDS-PAGE of avidin from the cleavage reaction with F-1.	40
Figure 32 SDS-PAGE of avidin from the cleavage reaction with F-2.	41
Figure 33 SDS-PAGE of avidin from the cleavage reaction with F-3.	41
Figure 34 SDS-PAGE of avidin from the cleavage reaction with fluorescein derivatives.	42
Figure 35 The cleavage yields of peptide fragments from the photoreaction of avidin with fluorescein derivatives.	42
Figure 36 Cleavage pattern of lysozyme from the photoreaction with three probes.	43
Figure 37 Cleavage pattern of avidin from the photoreaction with F-1 and F-2.	44

Figure 38 Absorption spectra of (a) F-1, (b) F-2 and (c) F-3 in the absence and presence of lysozyme.....	46
Figure 39 Absorption spectra of (a) F-1, (b) F-2 and (c) F-3 in the absence and presence of avidin.	48
Figure 40 The Stern-Volmer quenching plots of F-1 (a), F-2 (b) and F-3 (c) by titration with CoHA (0-1 mM), in the absence and presence of protein (lysozyme or avidin).	50
Figure 41 The structure of F-1 docked to lysozyme.	52
Figure 42 The structure of F-2 docked to lysozyme.	53
Figure 43 The structure of F-3 docked to lysozyme.	54
Figure 44 The structure of F-1 docked to avidin.....	56
Figure 45 The structure of F-2 docked to avidin.....	57
Figure 46 The structure of F-3 docked to avidin.....	58
Figure 47 Structure of $\text{MoO}(\text{O}_2)_2(\text{asparagine})(\text{H}_2\text{O})$: Mo-asn.	60
Figure 48 SDS-PAGE of pepsin from the cleavage reaction with Mo-asn.	61
Figure 49 The cleavage yields of peptide fragments from the photoreaction of pepsin with Mo-asn.	62
Figure 50 SDS-PAGE of pepsin from the thermal reaction with Mo-asn.	63
Figure 51 SDS-PAGE of pepsin from the thermal reaction with Mo-asn.	64
Figure 52 The cleavage yields of peptide fragments from the thermal reaction of pepsin with Mo-asn.	64
Figure 53 SDS-PAGE of pepsin from the cleavage reaction with Mo-asn.	65
Figure 54 The cleavage yields of peptide fragments by thermal reaction of pepsin and Mo-asn.....	66
Figure 55 Cleavage pattern of BSA from photoreaction with PMA-IB.....	68

Figure 56 Cleavage patterns of pepsin from photoreaction (a) and thermal reaction (b) with Mo-asn.	70
Figure 57 SDS-PAGE of β -lactoglobulin B from the cleavage reaction with F-1.	77
Figure 58 SDS-PAGE of concanavalin A from the cleavage reaction with F-1.	77
Figure 59 SDS-PAGE of BSA from the cleavage reaction with F-1.	78
Figure 60 SDS-PAGE of HSA from the cleavage reaction with F-1.	78
Figure 61 SDS-PAGE of β -lactoglobulin B from the cleavage reaction with F-2.	79
Figure 62 SDS-PAGE of concanavalin A from the cleavage reaction with F-2.	79
Figure 63 SDS-PAGE of BSA from the cleavage reaction with F-2.	80
Figure 64 SDS-PAGE of HSA from the cleavage reaction with F-2.	80
Figure 65 SDS-PAGE of β -lactoglobulin B from the cleavage reaction with F-3.	81
Figure 66 SDS-PAGE of concanavalin A from the cleavage reaction with F-3.	81
Figure 67 SDS-PAGE of BSA from the cleavage reaction with F-3.	82
Figure 68 SDS-PAGE of HSA from the cleavage reaction with F-3.	82

CHAPTER 1

INTRODUCTION

Background

Proteins are significant biomolecules that display variety biological functions in cells. The diverse biological functions in proteins are the results of many variations in amino acid composition and sequences in proteins (Boyer, 2002). Therefore, the study on sequencing information of amino acid residues will be important to obtain more understanding of the structure and function of proteins. Since the direct result of the amino acid sequencing in protein or long chain polypeptide cannot be directly determined (Voet, Voet, & Pratt, 2013) and the peptide bond is extremely stable (half life of ~ 7 years at room temperature, pH 7) (Kahne & Skill, 1988), the development of site-specific protein cleaving reagents will be very useful. In general, selective cleavage of protein can be achieved by binding the chemical reagent to the target protein at specific site and subsequent activation with light (photo reaction) or heat (thermal reaction) to cleave the protein backbone. The chemical reagents that can cleave protein at specific site can be useful as biochemical tools (Kumar et al., 1998). For example, these reagents can be utilized to produce smaller peptides for amino acid sequencing, understanding of the interaction between small molecules and proteins and designing of novel therapeutic agents (Buranaprapuk, Kumar, Jockusch, & Turro, 2000; Ghaim, Greiner, Meares, & Gennis, 1995; Hoyer, Cho, & Schultz, 1990).

In general, the protein cleaving reagents can be divided into two major classes: (1) organic molecules, and (2) metal complexes (inorganic molecules). Designing of both types of molecules have been developed for the cleavage of proteins in our laboratory. Using organic molecules, the molecules should consist of a suitable recognition element for binding to the target site on the protein and a reactive group which can be activated to initiate the cleavage reaction (Buranaprapuk, Malaikaew, Svasti, & Kumar, 2008). Py-Phe, for example, was designed for cleavage of proteins (lysozyme and BSA) under photoreaction. Py-Phe was synthesized by linking the specific recognition element (phenylalanine) with pyrenyl chromophore. This reagent

cleaved lysozyme between Trp 108 - Val 109, while BSA was cleaved between Leu 346 - Arg 347 (Kumar & Buranaprapuk, 1997). In addition, short peptides and specific substrates also have been used as a recognition element to attach to pyrenyl chromophore, such as Py-(Gly)_n-Phe ($n = 1, 2$), Py-Phe-Gly-Gly (Kumar & Buranaprapuk, 1999) and Py-biotin (Malaikaew, Svasti, Kumar, & Buranaprapuk, 2011) for exploring the role of functional group of the probe side chain in the protein binding and photocleavage reaction. The side chain in the probe structure has shown an important role on the efficiency and selectivity of the cleavage reaction. From the important role of the probe side chain, this study developed the new designed chemical reagents for exploring the binding and photocleavage properties on proteins by attaching the specific recognition element (ibuprofen) to the pyrenyl chromophore. Moreover, investigation of photocleavage properties of fluorescein derivatives as fluorescent probes is also explored for initiation of the protein cleavage reaction. Fluorescein is a common fluorophore that have been widely utilized as a fluorescent probe in biological and medical applications (Sulaiman, Kulathunga, & Abou-Zied, 2015). Fluorescein shows very high molar extinction coefficient at the absorption wavelength near 490 nm and high quantum yield in the emission wavelength region (480 - 600 nm) (Abou-Zied & Sulaiman, 2014), while proteins do not absorb and emit the light in these regions. The interference of protein absorption and fluorescence does not affect for initiation of the photocleavage reaction by fluorescein. Therefore, in the current studies, fluorescein has been selected as a reactive group for initiation of the protein cleavage reaction in the molecular design.

In another way, attachment of the metal complex to specific site on protein is one approach that has been proven to be successful for cleavage of protein at specific site (Rana & Meares, 1991). In the previous researches, many metal complexes, such as cobalt (III) complexes, have shown significant artificial metallopeptidase activities for cleavage of protein at specific site under thermal conditions (Kumar, Buranaprapuk, Cho, & Chaudhari, 2000). These complexes can cleave lysozyme between Ala 110 – Trp 111 under mild conditions (neutral pH, 37 °C). In addition, the ability of metal complexes

for cleavage of proteins at specific site under photo conditions also have been demonstrated, for example, cobalt (III) (Kumar & Thota, 2005) and molybdenum (VI) complexes (Jityuti, Liwporncharoenvong, & Buranaprapuk, 2013). Therefore, this research focused on the study of the protein cleavage properties of the new designed probes (PMA-IB), fluorescein derivatives and metal complex (molybdenum complex). The binding affinity and binding location of these probes on the proteins have been investigated here.

Objectives of the study

1. To design and synthesize of new chemical reagent for site-specific cleavage of proteins.
2. To study the cleavage of proteins by the new designed chemical reagent, fluorescein derivatives and metal complex.
3. To determine the binding affinity and to investigate the binding location of the chemical reagents on the proteins.

Significance of the study

1. To obtain the new protein cleaving reagents.
2. To obtain the appropriate conditions for the protein cleavage reaction.
3. To obtain the binding affinity and specific cleavage site on the proteins.

Scope of the study

1. Synthesis and characterization of new designed chemical reagents.
2. Study of the cleavage of protein by using SDS-PAGE (sodium dodecylsulfate - polyacrylamide gel electrophoresis).
3. Investigation of the specific cleavage site on proteins by using Edman degradation technique.
4. Determination of the binding affinity of the chemical reagents to the proteins by using spectroscopic methods.

5. Determination of the binding location of the chemical reagents on the proteins by using molecular docking.



CHAPTER 2

REVIEW OF THE LITERATURE

In this chapter, research papers and related research on the interaction between protein and small molecule will be presented on the topics below.

1. Proteins
2. Cleavage of protein
3. Spectroscopic methods
4. Computational chemistry
5. Related research

1. Proteins

Proteins are important biological macromolecules in human life. A protein is built from a set of 20 amino acids. The general structure of these amino acids is composed of a hydrogen atom, an amino group, a carboxyl group and a side chain (R group), connected to the carbon center (α -carbon) (Figure 1). Each of amino acid has different properties from others in the side chains (Boyer, 2002; Nelson & Cox, 2008).

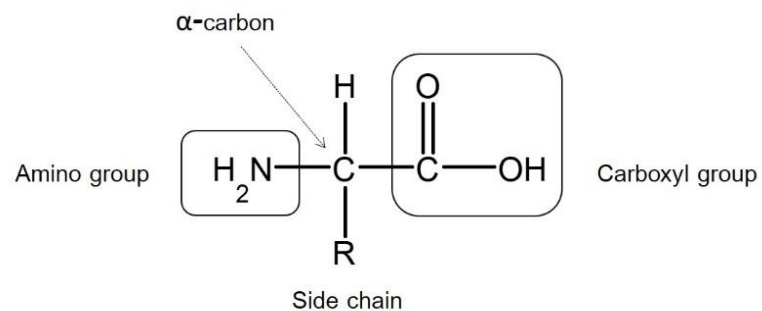


Figure 1 Basic structure of amino acid.

Amino acid residues can be conjugated to form peptides and proteins by peptide bonds. A linkage is built by the carboxyl group of one amino acid cooperated with an amino group of another amino acid, with the release of a molecule of water (Figure 2), (Boyer, 2002; Nelson & Cox, 2008)

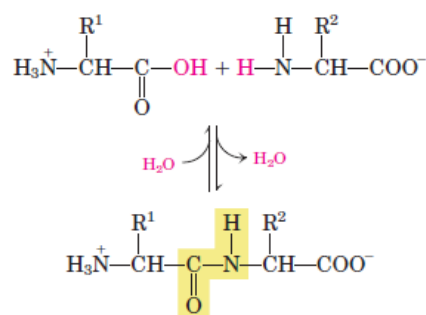


Figure 2 Formation of a peptide bond.

Source: Nelson, D. L., & Cox, M. M. (2008). *Lehninger principles of biochemistry*.

The structure of 10 to 100 amino acids are linked together. This structure is called a polypeptide. When more than 100 amino acids are joined, the product is called a protein (Boyer, 2002). The different biological activities in cells are generally caused by containing thousands of different proteins in cells (Nelson & Cox, 2008). Therefore, the studies on a protein in detail are essential to obtain more understanding on the protein structure and function.

2. Cleavage of protein

The interactions between protein and various small molecules have been of interest in many biological processes because of their importance in the explanation of the protein structure and function (Buranaprapuk & Kumar, 2018; Kumar, Buranaprapuk, & Thota, 2002). One approach to study this interaction is to design a chemical reagent that can directly bind to a protein at specific site and cleave the peptide bond upon activation with light or heat (Buranaprapuk et al., 2008; Kumar & Buranaprapuk, 1999).

Chemical reagents that can cleave peptides and proteins at specific sites under mild conditions are of interest as potential artificial peptidases for applications in biological chemistry. These reagents are utilized for the understanding of biomolecular recognition with small molecules and for creating smaller fragments that more amenable for amino acid sequencing (Buranaprapuk et al., 2000). Site specific cleavage of protein with a chemical reagents has been reported in our laboratory such as pyrenyl derivatives (Buranaprapuk et al., 2008; Kumar et al., 1998) or metal complexes (Kumar et al., 2000; Kumar & Thota, 2005). In general, the progress of the protein cleavage into smaller peptide fragments can be monitored by gel electrophoresis (SDS-PAGE) experiments and the peptide fragments from the gels can be isolated and analyzed to obtain amino acid sequence for investigation of the location of cleavage site on the protein (Jityuti et al., 2013).

2.1 SDS-polyacrylamide gel electrophoresis (SDS-PAGE)

SDS-polyacrylamide gel electrophoresis (SDS-PAGE) of protein is a common technique to separate protein in polyacrylamide gel. When addition of the detergent SDS (sodium dodecyl sulfate) to proteins, SDS can bind to protein in a ratio of about one SDS molecule for every two residues of amino acid. Because of the negative charge of SDS molecule (Figure 3), the net charge of SDS-bound protein is negative with similar shapes. Therefore, the separation of protein by SDS-PAGE depends only on molecular weight, with mobility of smaller protein (polypeptide) moving more rapidly than larger protein (Nelson & Cox, 2008; Ninfa & Ballou, 1998; Voet et al., 2013).

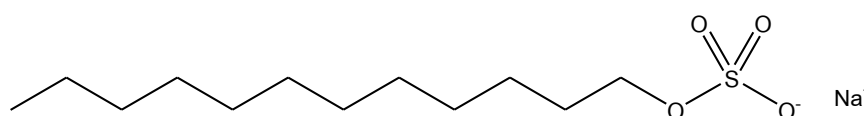


Figure 3 Structure of sodium dodecyl sulfate (SDS).

After electrophoresis, the fragment of protein can be visualized by immersing the gel in a solution of a dye (Coomassie blue). This technique can determine the molecular weight of an unknown protein by comparing the band position of the unknown protein with the band positions of standard proteins (known molecular weights) in the same gel. The molecular weight of an unknown protein can be estimated to a good approximation from its position in the gel (Moran, Horton, Scrimgeour, & Perry, 2014; Nelson & Cox, 2008).

2.2 Edman degradation of peptide sequencing

Edman degradation is a chemical technique invented by Pehr Edman. This technique can be utilized to determine the sequence of amino acids in peptide fragments. In this process, the amino group at the N-terminus of a peptide reacts with phenyliso-thiocyanate (PITC) to form a phenylthiocarbamoyl (PTC) adduct. After that, the N-terminal amino acid residue of the PTC adduct is cleaved by treating in anhydrous trifluoroacetic acid and converted to anilinothiazolinone (ATZ) derivative. The ATZ derivative residue can be extracted with organic solvent and treated with aqueous acid to a more stable phenylthiohydantoin (PTH) derivative. Then, this PTH derivative (PTH-amino acid) is identified by chromatography. After identification of the N-terminal amino acid residue, this procedure can be repeated in another cycle to identify the new N-terminal amino acid residue in polypeptide chain with the same reaction (Nelson & Cox, 2008; Voet et al., 2013).

3. Spectroscopic methods

Spectroscopic technique can be used to study the binding mechanism (binding constants, quenching constants) of protein with various small molecules. The information of the binding mechanism between protein and various small molecules (ligands) will help us to achieve better understanding on the biological processes (Rub, Khan, Asiri, Khan, & ud-Din, 2014).

3.1 Binding studies

The effect of protein on the absorption spectra of small molecules can be used to explore the binding mechanism of small molecules to the protein (Sulaiman et al., 2015). The absorption spectral data were used to calculate for the binding constants of small molecules bound to protein, which can be obtained from the Scatchard equation (equation 1) (Scatchard, 1949).

$$r/C_f = K_b(n-r)$$

Where r is the number of moles of small molecules bound per mole of protein, C_f is the concentration of the free small molecules, K_b is the binding constant and n is number of binding sites per protein. In equation 1, the binding constant is obtained from the slope of the plot of r/C_f as a function of r (Kumar & Buranaprapuk, 1999; Kumar, Buranaprapuk, Sze, Jockusch, & Turro, 2002).

3.2 Fluorescence quenching studies

Fluorescence quenching measurements is a useful method to study the interactions of small molecules with protein. This measurements can determine the accessibility of the quencher to the fluorophore at protein binding site, which can help us to understand the protein-ligand binding mechanism (Barbero et al., 2009; Kumar & Buranaprapuk, 1999; Malaikaew et al., 2011).

The fluorescence quenching data can be used to analyze the quenching constant by using the Stern-Volmer equation (equation 2) (Stern & Volmer, 1919).

$$I_0/I = 1 + K_{sv}[Q]$$

Where I_0 and I are the fluorescence intensity in the absence and presence of the quencher, respectively, $[Q]$ is the quencher concentration and K_{sv} is the Stern-Volmer quenching constant. According to the equation 2, the plot of I_0/I against $[Q]$ can provide the quenching constant (C.V. Kumar et al., 2002; Malaikaew et al., 2011).

4. Molecular docking

In order to understand the protein-ligand interactions, the knowledge of the binding site of ligand on protein is very important. One approach for the study of this interaction has been predicated base on molecular docking method. Molecular docking is an important method to apply for the interaction between protein and ligand. This technique can be used to predict the binding location and binding affinity of ligand within the protein (Elokely & Doerksen, 2013; Zheng et al., 2013). In addition, this method is widely used for the study in the drug design (Zheng et al., 2013). Therefore, in this research study, the binding location of various small molecules in protein were explored by using molecular docking method.

5. Related research

Developing of the new chemical reagents for cleavage of proteins has been interested in biological chemistry. These chemical reagents can help us for gaining better understanding of the interactions between small molecules and proteins (Kumar & Buranaprapuk, 1999). Therefore, the work in this study were related to the development of protein cleaving reagents. A major class of chemical reagents for cleavage of proteins described here will include: (1) pyrene derivatives, (2) fluorescein derivatives and (3) metal complexes.

5.1 Pyrene derivatives

The designed photochemical reagents to cleave proteins should consist of a recognition element for binding to the specific site on the protein and a chromophore which can be activated to initiate the photocleavage reaction (Buranaprapuk & Kumar, 2018). In the previous study, many researchers have selected pyrene as a chromophore in the modular design because pyrene has high extinction coefficient at 340-350 nm and a long-lived high energy excited state for photoreaction to occur (Kumar et al., 1998). For example, in 1997, Kumar and Buranaprapuk proposed a method to design and synthesize a new selective chemical reagent (Py-Phe) (Figure 4) for photocleavage of model proteins (lysozyme and BSA). In the study, an amino acid, phenylalanine, was

used as a recognition element to covalently attach to the pyrenyl chromophore. In addition, phenylalanine has a carboxyl group which provide the hydrophilicity, while the pyrenyl chromophore is hydrophobic. Therefore, binding of Py-Phe at the hydrophobic binding site on the protein which was near the hydrophilic residues could provide more selectivity than binding at hydrophobic or hydrophilic site alone. This chemical reagent could cleave lysozyme at specific site between Trp 108 - Val 109, while the cleavage site of BSA occurred between residues Leu 346 - Arg 347 (Kumar & Buranaprapuk, 1997).

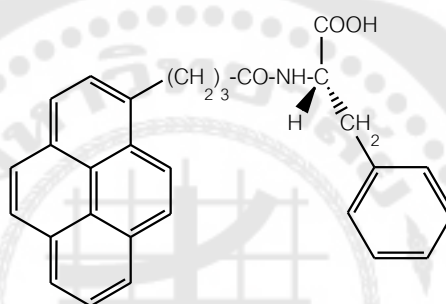


Figure 4 Structure of Py-Phe.

In 1998, Kumar and coworkers studied the binding properties of Py-Phe upon binding to the proteins (lysozyme and BSA). Py-Phe bound to lysozyme with binding constant of $2.2 \pm 0.3 \times 10^5 \text{ M}^{-1}$, whereas binding to BSA indicated the binding constant of $6.5 \pm 0.4 \times 10^7 \text{ M}^{-1}$. The hydrophobic segment of Py-Phe bound to the interior region of BSA, while the hydrophilic group anchored the nearby charged residues of amino acids in that region on the protein (Figure 5b). However, the binding mode for lysozyme was different. The probe seemed to bind to lysozyme at the surface of the protein (Figure 5a). The differences in the binding properties between Py-Phe and these two proteins could provide the scope for designing new chemical reagents for selectively binding to the proteins and perhaps for the protein cleavage in the future (Kumar et al., 1998).

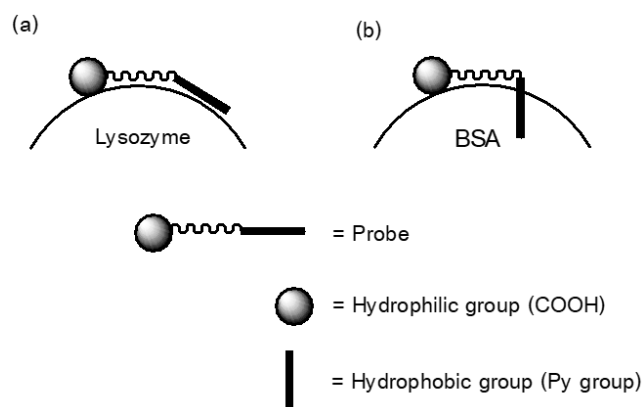


Figure 5 Binding properties of the probe on protein (a) lysozyme and (b) BSA.

In 1999, Kumar and Buranaprapuk designed an analog of pyrene derivatives (Py-Gly, Py-(Gly)_n-Phe ($n = 0, 1, 2$) and Py-Phe-Gly-Gly) (Figure 6) for investigation of the protein photocleavage properties. From the study, the data clearly demonstrated the cleavage efficiency and selectivity of the probe upon binding to the protein. The linker length between the pyrenyl group and the carboxyl terminus in the probe structure have shown an important role on the efficiency and selectivity of the cleavage reaction (Kumar & Buranaprapuk, 1999).

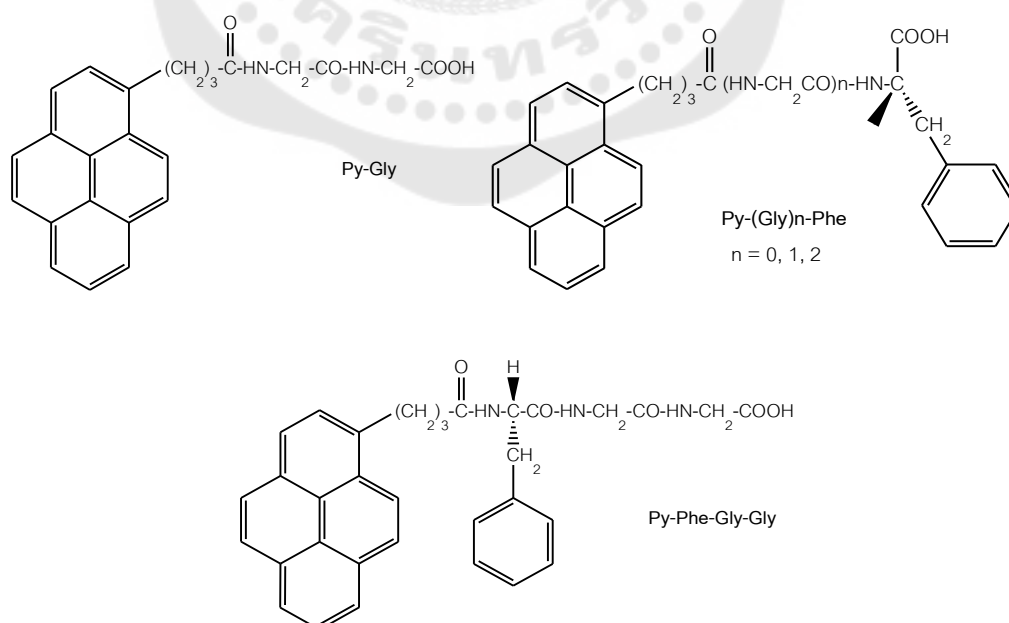


Figure 6 Structures of the Py-Phe analogs.

In 2000, Buranaprapuk and coworkers synthesized the pyrenyl peptides (Py-Gly-X; when X = phenylalanine, tyrosine, tryptophan and histidine) for exploring the role of specific amino acid residues on the probe in the photocleavage reaction. These pyrenyl peptide probes were synthesized by attaching different amino acid residues to the probe side chain of 4(1-pyrenyl) butyric acid (Figure 7).

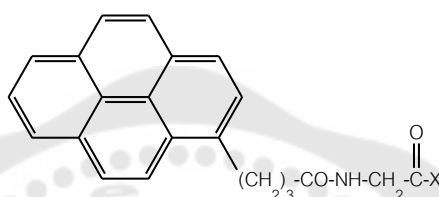


Figure 7 Structures of pyrenyl peptides: Py-Gly-X, where X = phenylalanine (Py-Gly-Phe), tyrosine (Py-Gly-Tyr), tryptophan (Py-Gly-Trp), and histidine (Py-Gly-His).

This study indicated that Py-Gly-Phe and Py-Gly-His cleaved BSA and lysozyme at similar sites, compared to the results obtained with Py-Phe under the same photo conditions, while Py-Gly-Tyr and Py-Gly-Trp analogs did not yield any fragmentation of these two proteins (Buranaprapuk et al., 2000).

In addition, in 2011, Malaikaew and coworkers have developed the new pyrenyl probe by attaching the specific recognition element to the pyrenyl chromophore. Biotin was chosen for the specific recognition element because biotin was known to bind to avidin with high binding constant (10^{15} M^{-1}). In this study, d-biotinyl-1(1-pyrene)methylamide (Py-biotin) (Figure 8) was designed and synthesized for site specific photocleavage of avidin. When the mixture of Py-biotin and avidin was irradiated at 342 nm (Py-biotin absorption band), in the presence of an electron acceptor (CoHA), the result showed that, avidin was cleaved between Thr 77 and Val 78 (Malaikaew et al., 2011).

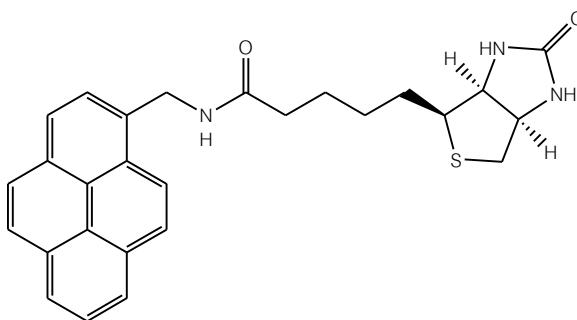


Figure 8 Structure of Py-biotin.

From the above research studies, these results are referred to (1) the ability of pyrenyl chromophore to strongly absorb the light at specific wavelength to initiate the photoreactions and (2) the important role of the side chain in the probe structure for anchoring the protein at specific region. Therefore, in this proposed study, a new chemical reagent was designed and synthesized, based on the mechanisms in the previous studies, by attaching a known recognition element such as ibuprofen, to the pyrenyl chromophore for exploring the photocleavage and spectroscopic properties with protein.

Ibuprofen (Figure 9) is a non-steroidal-anti-inflammatory-drug (NSAID) that is widely used for treating inflammation (Jasinska, Ferguson, Mohamed, & Szreder, 2009; Li & Yao, 2009).

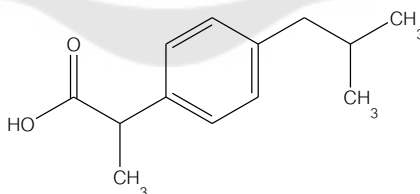


Figure 9 Structure of ibuprofen.

In addition, many researchers have used ibuprofen as a site marker for competitive experiments between small molecules and serum albumin (Shahabadi, Khorshidi, & Moghadam, 2013; Zhang, Ni, & Kokot, 2010) because ibuprofen is known to bind to the sub-domain IIIA (site II) of serum albumin (Figure 10) (Yamasaki, Chuang,

Maruyama, & Otagiri, 2013) with binding constant in the range of $10^5 - 10^6 \text{ M}^{-1}$ (D'Alessandro, Ellis, Carter, Stock, & March, 2013; Zhang et al., 2010). Thus, in this research, ibuprofen was used as a recognition element to target the binding site on serum albumin.

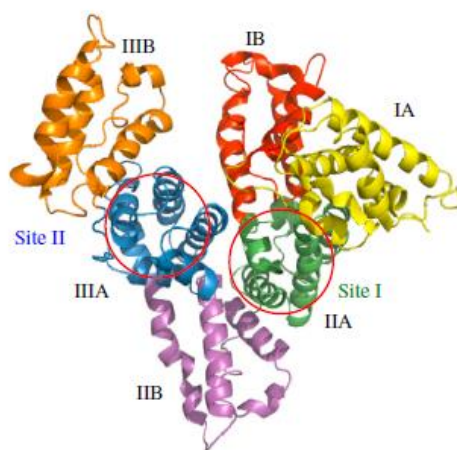


Figure 10 Crystal structure of HAS.

Source: Yamasaki, K., Chuang, V. T., Maruyama, T., & Otagiri, M. (2013).

Albumin-drug interaction and its clinical implication. p. 5439.

5.2 Fluorescein derivatives

Fluorescein and its derivatives are widely utilized as a fluorescent probe in biological and medical applications because of its high molar extinction coefficient at the wavelength near 490 nm and high fluorescence quantum yield (Abou-Zied & Sulaiman, 2014; Sulaiman et al., 2015). In previous research, many researchers have studied the interaction of proteins with fluorescein and its derivatives. The example of publications to these studies are summarized here.

In 1999, Kada and coworkers synthesized the new biotin-fluorescein conjugate (biotin-4-fluorescein and biotin-4-FITC, Figure 11) for investigation of the binding properties of these probes upon binding to avidin and streptavidin. These probes bound to avidin and streptavidin with high affinity, fast association and non-

cooperative binding with proteins, which is useful for quantitation of avidin and streptavidin (K. Gerald, Heinz, & Hermann, 1999; K. Gerald, Karl, Heinz, & Hermann, 1999).

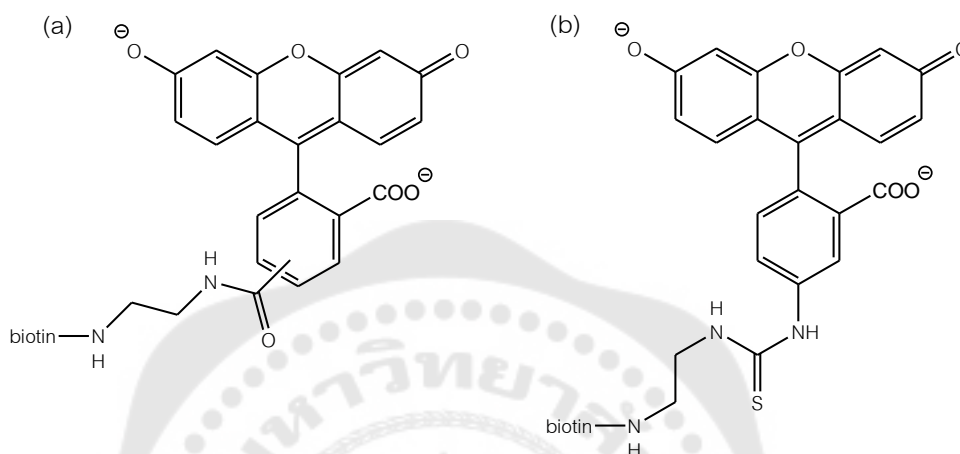


Figure 11 Structures of (a) biotin-4-fluorescein and (b) biotin-4-FITC.

In 2009, Barbero and coworkers have studied the protein binding of fluorescein sodium salt (Figure 12) with the different bovine serum albumin (BSA) grades of purity. The BSA binding properties were determined by the quenching of BSA fluorescence in the presence of fluorescein sodium salt. These results can explore the effect of the grade of purity on BSA-ligand binding. BSA binding properties differed depending on different BSA grades of purity (Barbero et al., 2009).

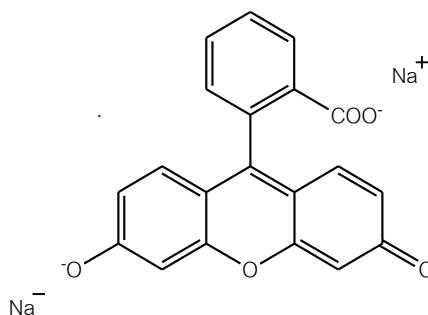


Figure 12 Structure of fluorescein sodium salt.

In 2012, Yadav and coworkers have investigated the interaction of fluorescein with protein (BSA) by using spectroscopic method. In this study, fluorescein bound to BSA with binding constant of $2.1 \pm 0.2 \times 10^5 \text{ M}^{-1}$. In addition, site marker competitive experiment and molecular docking study were used to explain the binding location of fluorescein on proteins. The data indicated that fluorescein preferred to bind to the surface of the proteins (non-specific binding) (Yadav, Das, & Sen, 2012).

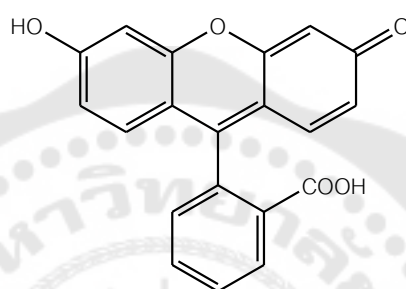


Figure 13 Structure of fluorescein.

In addition, in 2014, the binding mechanism of fluorescein on protein (HSA) has been characterized by using spectroscopic method. The results in this study indicate that fluorescein can bind to site I (or warfarin site) of HSA with a moderate strength ($K = 10000 \text{ M}^{-1}$). The data of this study can be useful for many applications of using fluorescein as a fluorescent probe in biology and medicine (Abou-Zied & Sulaiman, 2014).

The previous research studies of interaction between fluorescein (and its derivatives) and proteins have clearly demonstrated the binding properties of fluorescein and its derivatives with proteins, but no research has used fluorescein and its derivatives as protein cleaving reagents. Therefore, the study of the photocleavage properties of fluorescein and its derivatives on proteins was interesting.

5.3 Metal complexes

The ability of metal complexes as protein cleaving reagents has been known. A general procedure for cleavage of proteins by metal complexes under photochemical reaction is outlined in Figure 14 (Jyotsna, Kumar, Jockusch, & Turro, 2010). In step 1, metal complex binds to a protein at specific site and can cleave the protein at this corresponding site upon activation by light in the step 2.

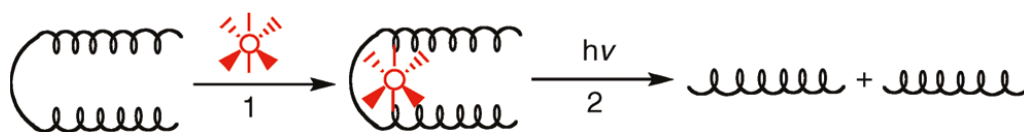


Figure 14 General procedure for cleavage of protein by metal complexes.

Source: Jyotsna, T., Kumar, C. V., Jockusch, S., & Turro, N. J. (2010). Steady-state and time-resolved studies of the photocleavage of lysozyme by Co (III) complexes. p. 1966.

In 2005, Kumar and Thota reported the first report of protein photocleavage by metal complexes. This study demonstrated the ability of Co (III) complexes (Figure 15) for cleaving lysozyme at specific site under photochemical conditions. These metal complexes can cleave lysozyme between Trp108 - Val109. No cleavage was detected in the absence of the Co(III) complexes or the light (Kumar & Thota, 2005).

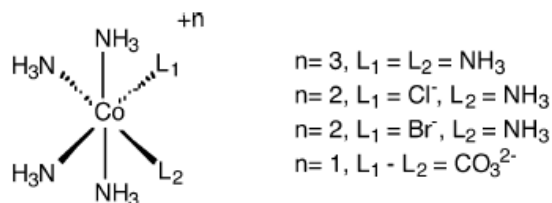


Figure 15 Structures of Co (III) complexes.

In 2013, the photocleavage of protein by molybdenum complex has been reported for the first time. A molybdenum complex (molybdenum (VI) peroxy α -amino acid complex) was synthesized by attaching amino acid (leucine) residue to molybdenum trioxide (MoO_3) (Figure 16). This metal complex can be utilized to cleave porcine pepsin under photochemical conditions without the use of other chemical reagents (Jityuti et al., 2013).

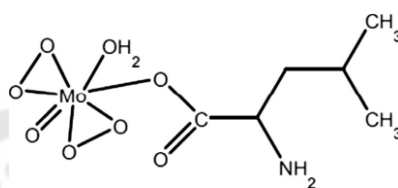


Figure 16 Structure of $\text{MoO}(\text{O}_2)_2(\alpha\text{-leucine})(\text{H}_2\text{O})$.

In addition, in 2015, the molybdenum (VI) peroxy α -amino acid complexes, $\text{MoO}(\text{O}_2)_2(\alpha\text{-aa})(\text{H}_2\text{O})$ (aa = leucine, glutamine and glycine) have been designed and used for site specific cleavage of pepsin under thermal condition. These three synthesized molybdenum complexes can cleave pepsin at different cleavage sites, indicating that the selectivity of the probe (molybdenum complexes) on protein depends on the charges and the lengths of the amino acid side chains attached to molybdenum (Jityuti, Buranaprapuk, & Liwporcharoenvong, 2015).

From the ability of metal complexes for protein cleavage upon activation by light or heat, this research focused on the investigation of the cleavage of proteins under photo and thermal conditions by new molybdenum (VI) peroxy α -amino acid complex.

CHAPTER 3

METHODOLOGY

1. Equipment

- Precision analytical balance digital scale, Mettler Toledo, code AB104-S
- Magnetic stirrer, GEM, code MS-115
- TLC plate, Merck
- Rotary evaporator, Buchi, code R-210
- Micropipette (2, 20, 100, 200 and 1000 μL), Gilson
- pH meter, Mettler Toledo
- Cavitator ultrasonic cleaner, Mettler electronics Corp.
- Flexi Dry, FTS systems
- Blot Filter paper, BIO-RAD
- Sequi-Blot™ PVDF membrane (2 μm), BIO-RAD
- Mini Trans-Blot® Electrophoretic Transfer Cell, BIO-RAD
- SDS – PAGE apparatus, BIO-RAD
- UV-spectrophotometer, Shimadzu, code UV-2401 PC
- Fluorescence spectrophotometer, Jasco, code FP-8300 (PC)

2. Chemical reagents

- 1-pyrenemethylamine hydrochloride (PMA), Sigma-Aldrich
- 2-(4-Isobutylphenyl) propionic acid (Ibuprofen), TCI
- 1-hydroxybenzotriazole (HoBt), TCI
- Dimethylformamide (DMF), Labscan
- N, N-diisopropylethylamine (DIPEA), Sigma-Aldrich
- 1-(3-dimethylaminopropyl)-3-ethylcarbodiimide hydrochloride (EDC), TCI
- Ethyl acetate, Labscan
- Hydrochloric acid (HCl), Labscan
- Sodium bicarbonate (NaHCO_3), Labscan
- Sodium chloride (NaCl), Labscan

- Sodium sulphate anhydrous (Na_2SO_4), Labscan
- Dichloromethane (DCM), Labscan
- Hexane, Labscan
- Molybdenum trioxide (MoO_3), Carlo Erba
- Hydrogen peroxide (H_2O_2), Carlo Erba
- Amino acid, Sigma-Aldrich
- Proteins, Sigma-Aldrich
- Trizma® hydrochloride, Sigma-Aldrich
- Ascorbic acid, Sigma-Aldrich
- Cobalt (III) hexamine trichloride [$\text{Co}(\text{NH}_3)_6\text{Cl}_3 : \text{CoHA}$], Sigma-Aldrich
- Acrylamide, Plusone
- Methylenebisacrylamide, Plusone
- Glycerol, Fluka
- Trizma® base, SAFC
- Sodium dodecyl sulfate (SDS), Sigma-Aldrich
- Ammonium persulfate, Sigma-Aldrich
- Tetramethylethylenediamine (TMEDA or TEMED), Sigma-Aldrich
- Sodium dodecyl sulfate (SDS), Sigma-Aldrich
- Bromophenol Blue, Plusone
- 2-Mercaptoethanol, Merck
- Tricine, Sigma-Aldrich
- Mark 12™ MW Standard, Invitrogen
- Coomassie blue R-250, Sigma-Aldrich
- Methanol, Fisher chemical
- Acetic acid, Carlo Erbra
- Deionized water
- Cyclohexylaminopropane sulfonic acid (CAPS), Sigma-Aldrich
- Fluorescein and its derivatives, Sigma-Aldrich

3. Methods

3.1 Synthesis of chemical reagents

3.1.1 Synthesis of pyrene derivative (PMA-IB)

A solution of N, N-diisopropylethylamine (DIPEA) (0.52 mL, 3 mmol) and 1-(3-dimethyl-aminopropyl)-3-ethylcarbodiimide hydrochloride (EDC) (0.60 g, 3 mmol) was added to a solution of 1-pyrenemethylamine hydrochloride (0.27 g, 1 mmol), ibuprofen (0.27 g, 1.3 mmol) and 1-hydroxybenzotriazole (HoBt) (0.41 g, 3 mmol) in dimethylformamide (20 mL). The solution mixture was then stirred at -20 °C under nitrogen atmosphere for 20 min before warming to room temperature and the solution was kept stirring at room temperature for overnight. Water was added to the mixture and the solution was extracted with ethyl acetate. The organic layer was collected and washed with hydrochloric acid (10%), water, saturated sodium bicarbonate solution, saturated sodium chloride solution and dried over sodium sulfate anhydrous. The solvent was then evaporated, and the resulting residue was purified by silica gel column chromatography (ethyl acetate/hexane, 7/3, v/v) to give the product compound as a white solid (0.41 g, 95%).

3.1.2 Synthesis of $\text{MoO}(\text{O}_2)_2(\text{asparagine})(\text{H}_2\text{O})$

Molybdenum complex with the structure of $\text{MoO}(\text{O}_2)_2(\text{asparagine})(\text{H}_2\text{O})$ was prepared by following the previously reported procedures (Djordjevic, Vuletic, Jacobs, Renslo, & Sinn, 1997). This molybdenum complex was synthesized by dissolving molybdenum trioxide (MoO_3) in 30% H_2O_2 and the solution was stirred at room temperature for 24 h. Then, asparagine was added to the above solution and the solution was kept stirring at room temperature for 24 h. The yellow crystals precipitate was obtained (yield: 72.36 %).

3.2. Protein cleavage experiments

3.2.1 Photocleavage of protein

In photochemical reagent, the mixture of chemical reagent (probe), protein and cobalt (III) hexamine trichloride $[\text{Co}(\text{NH}_3)_6\text{Cl}_3; \text{CoHA}]$, in 50 mM Tris-HCl buffer pH 7 (total volume 200 μL) was irradiated at the specific wavelength using 150 W xenon lamp. Light control sample was prepared with the same conditions, except that the mixture solution is prevented from light. In addition, protein photocleavage study was performed at various irradiation time. In case of metal complex, the solution mixture of metal complex (probe) and protein was irradiated at 320 and 340 nm with 150 W xenon lamp.

3.2.2 Thermal cleavage of protein

A mixture of the chemical reagent (probe) and protein was incubated at 37 °C for 0-24 h in 50 mM Tris-HCl buffer pH 7 (total volume 200 μL). Heat control sample was prepared using the same conditions, except that the mixture solution is kept frozen after mixing. In addition, protein thermal cleavage study was performed at various concentrations of the chemical reagent and incubation time of reaction mixture.

3.3 Sodium dodecyl sulfate polyacrylamide gel electrophoresis (SDS-PAGE)

After preparation of reaction samples (as described above), all reaction mixtures were dried under reduced pressure and the dried samples were redissolved in loading buffer (A loading buffer solution was prepared by mixing SDS, glycerol, bromophenol blue R-250 and mercaptoethanol in 50 mM Tris-HCl, pH 6.8). After that, the sample solutions in the loading buffer were denatured by heating for 3 min and then analyzed by SDS-PAGE experiment, which is performed by following the literature procedure (Schagger & Jagow, 1987). The solutions in SDS-PAGE experiment were prepared as following.

3.3.1 Preparation of acrylamide/bisacrylamide solution (50.00 mL)

Acrylamide	23.25	g
Bisacrylamide	1.50	g

Acrylamide/bisacrylamide solutions were prepared by dissolving acrylamide and bisacrylamide in 50.00 mL of deionized water.

3.3.2 Preparation of gel buffer solution (50.00 mL)

Trizma [®] base	36.32	g
SDS	0.30	g

A gel buffer solution was prepared by dissolving Trizma[®] base and SDS in 50.00 mL of deionized water and then adjusted to pH 8.45 with 6M HCl.

3.3.3 Preparation of cathode buffer solution 5X (500.00 mL)

Trizma [®] base	6.05	g
Tricine	8.96	g
SDS	0.50	g

A cathode buffer solution 5X was prepared by dissolving Trizma[®] base, tricine and SDS in 500.00 mL of deionized water.

3.3.4 Preparation of anode buffer solution 5X (500.00 mL)

An anode buffer solution 5X was prepared by dissolving Trizma[®] base 12.20 g in 500.00 mL of deionized water and then adjusted to pH 8.9 with 6M HCl

The gels were run by applying a 60 V until the samples passed through the stacking gel, and then the voltage was increased to 110 V. On completion of the electrophoresis, the gels were stained with a staining solution and destained in 10% acetic acid. A staining solution was prepared by mixing of 0.5 % Coomassie blue (5 mL), acetic acid (10 mL) and methanol (50 mL) in 10% acetic acid (35 mL).

3.4 Western Blot (peptide transfer)

The peptide fragments on the gels were electroblotted to PVDF membrane using Mini Trans Blot cell (BIORAD). The preparation of chemical solution and PVDF membrane can be prepared as following:

3.4.1 Preparation of CAPS buffer solution 100 mM, pH 10.5 (1000.00 mL).

CAPS 22.13 g was dissolved in 1000.00 mL of deionized water and then adjusted to pH 10.5 with 1 M NaOH.

3.4.2 Preparation of a staining solution for PVDF membrane (100.00mL).

Coomassie blue R-250	0.10	g
Methanol	45.00	mL
Acetic acid	10.00	mL

Coomassie blue, methanol and acetic acid were mixed, and then adjusted the volume to 100.00 mL with deionized water.

3.4.3 Preparation of a destaining solution for PVDF membrane (100.00 mL).

Methanol	45.00	mL
Acetic acid	10.00	mL

Methanol and acetic acid were mixed, and then adjusted the volume to 100.00 mL with deionized water.

3.4.4 Preparation of PVDF membrane and the Blotting Filter Paper.

- PVDF membrane and the Blotting Filter Paper were cut to the size of a gel and soaked in methanol for 2-3 seconds.

- Blotting Filter Paper, PVDF membrane, Filter pad and gel were soaked in CAPS buffer for 10-15 min.

- The gel sandwiched (Figure 17a) was put into a buffer tank and connected to the power supply (Figure 17b) (Bio-Rad, 2017).

- The electrical current was adjusted to transfer peptide fragments.

- At completion of the run, the PVDF membrane was stained in staining solution for 2 min and rinsed with destaining solution for 1 min.

- The designed bands were cut and sent for amino acid analysis.

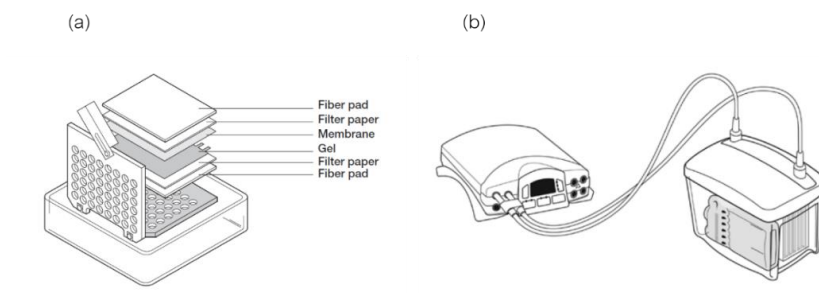


Figure 17 (a) Preparation of gel sandwich and (b) Mini Trans-Blot[®] Electrophoretic Transfer Cell.

Source: Bio-Rad. (2017). Mini Trans-Blot[®] Electrophoretic Transfer Cell Retrieved from www.bio-rad.com/webroot/web/pdf/lsr/literature/M1703930.pdf.

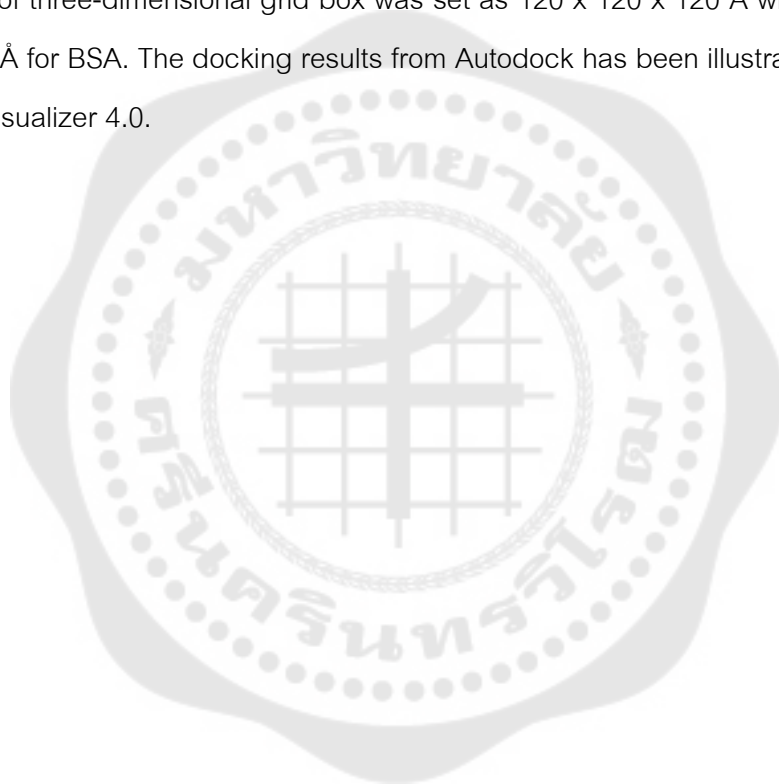
3.5 Spectroscopic method

In binding studies, UV–VIS spectroscopy is applied to estimate the binding constant of chemical reagent–protein complex formation. All absorption spectra were recorded using a Shimadzu UV-2401 PC UV–VIS spectrophotometer. The binding studies of the chemical reagents in the absence and presence of proteins were carried out in 50 mM Tris-HCl buffer pH 7 at room temperature. The solution of the chemical reagent was titrated with protein solution, and the spectral data were recorded in 300–600 nm region. The absorption spectral data were used for the calculation of the binding constant using the Scatchard equation (equation 1, chapter 2).

Fluorescence quenching studies were performed to estimate the quenching constant of chemical reagent–protein complex by cobalt (III) hexamine trichloride (CoHA) as a quencher. All fluorescence spectra were recorded on a Jasco FP-8300 spectrofluorometer. Measurement was performed by titrating the free chemical reagent and protein-bound chemical reagent with the CoHA. The fluorescence quenching data were analyzed by using the Stern-Volmer equation (equation 2, chapter 2) to investigate the quenching constant. A plot of I_0/I as a function of CoHA concentration can be constructed to estimate the quenching constant from the slope of the plot.

3.6 Molecular docking investigation

Autodock program (version 4.2) was utilized to predict the interaction between the protein and chemical reagents. Gaussian 03 package was used to prepare and optimize the structures of chemical reagents. The crystal structures of lysozyme (PDB ID: 4XAD), avidin (PDB ID: 1AVD) and BSA (PDB ID: 4F5S) were downloaded from Protein Data Bank (<http://www.rcsb.org/pdb>). The size of three-dimensional grid box was set as 100 x 100 x 100 Å with a grid spacing of 0.375 Å in lysozyme and avidin, and the size of three-dimensional grid box was set as 120 x 120 x 120 Å with a grid spacing of 0.703 Å for BSA. The docking results from Autodock has been illustrated by Discovery Studio Visualizer 4.0.



CHAPTER 4

FINDINGS

The main objective in this research has been focused on the study of the binding properties and the cleavage of protein by photochemical reagents and a metal complex. The binding affinity and binding location of these probes on the proteins were investigated using spectroscopic methods, SDS-polyacrylamide gel electrophoresis (SDS-PAGE) and molecular docking techniques. The frameworks for the study are as follows:

1. Pyrene derivative
 - 1.1 Synthesis and characterization of new pyrene derivative (PMA-IB)
 - 1.2 Cleavage of protein by PMA-IB
 - 1.3 Protein binding studies with PMA-IB
 - 1.4 Molecular docking studies of protein with PMA-IB
2. Fluorescein derivatives
 - 2.1 Cleavage of protein by fluorescein derivatives (F-1, F-2 and F-3)
 - 2.2 Peptide sequencing studies
 - 2.3 Protein binding studies with fluorescein derivatives
 - 2.4 Molecular docking studies of protein with fluorescein derivatives
3. Metal complex
 - 3.1 Synthesis of molybdenum complex (Mo-asn)
 - 3.2 Photocleavage of pepsin by Mo-asn
 - 3.3 Thermal cleavage of pepsin by Mo-asn

1. Pyrene derivative

1.1 Synthesis and characterization of new pyrene derivative (PMA-IB)

PMA-IB was synthesized by attaching ibuprofen to the pyrenyl chromophore, resulting in the white powder product (yield: 95%) (Figure 18). The product was characterized by $^1\text{H-NMR}$ and mass spectroscopy. $^1\text{H-NMR}$ (400 MHz, CDCl_3): 7.80-8.22 (m, 9H), 7.17 (d, 2H, $J = 7.6$ Hz), 7.02 (d, 2H, $J = 7.6$ Hz), 5.71 (bs, 1H), 5.08 (d, 2H, $J = 5.1$ Hz), 3.57 (q, 1H, $J = 7.0$ Hz), 2.38 (d, 2H, $J = 7.0$ Hz), 1.67-1.82 (m, 1H), 1.56 (d, 3H, $J = 7.2$ Hz), 0.80 (d, 6H, $J = 6.4$ Hz); HRMS (+ESI): 420.23 $[\text{M}+\text{H}]^+$.

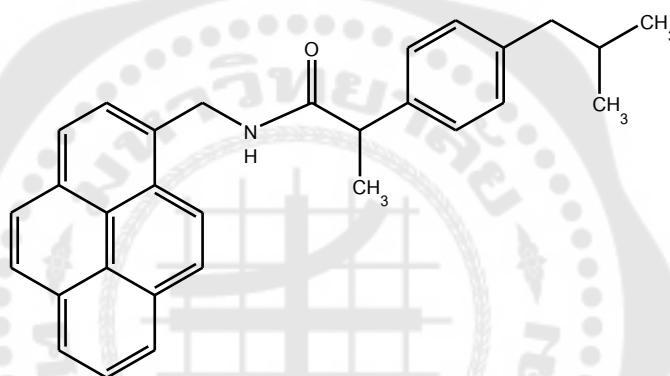


Figure 18 Structure of PMA-IB.

PMA-IB has absorption maxima at the wavelength of 351 nm (Figure 19).

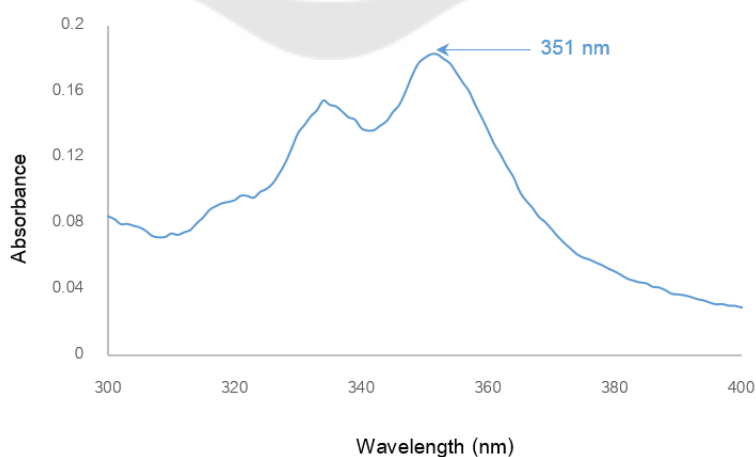


Figure 19 Absorption spectrum of PMA-IB (10 μM).

1.2 Cleavage of protein by PMA-IB

The selective cleavage of proteins by new pyrene derivative has been investigated in this study. This reaction can be achieved by binding the probe to the target site on protein and subsequent irradiation with light at specific wavelength initiate the photoreaction, resulting to the cleavage of the protein backbone. In the studies, the new designed chemical reagent (PMA-IB) was synthesized by attaching ibuprofen to the pyrenyl chromophore. Ibuprofen was use as a specific recognition element to target the binding site on serum albumin.

Photocleavage of BSA by PMA-IB was successful by irradiating the solution mixture of BSA, PMA-IB and an electron acceptor, cobalt (III) hexamine trichloride (CoHA), at 346 nm. The fragmentation of BSA was observed in SDS-polyacrylamide gel electrophoresis experiment (SDS-PAGE), as shown in Figure 20. BSA was cleaved by PMA-IB resulting in two new fragments as shown on the gel. When comparing the positions of new fragments with the positions of protein markers, the molecular weights of these fragments were calculated to approximately 45 and 22 kDa. No fragmentation of protein was discovered without PMA-IB, CoHA or light. The yields of the fragment bands obtained from the cleavage of BSA were determined by using ImageJ software (v 1.46r). The total cleavage yield of the new fragments (26.30%) was obtained when irradiating the solution mixture at 346 nm for 10 min, which was the highest yield of BSA from the photocleavage reaction with pyrenyl derivatives found in our laboratory.

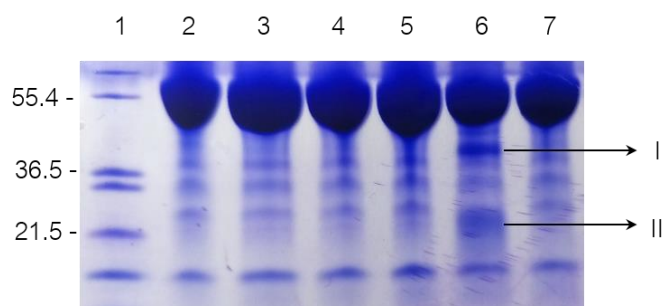


Figure 20 SDS-PAGE of the cleavage reaction of BSA with PMA-IB.

Lane 1: contained protein markers, indicated in kDa. Lane 2: contained BSA (15 μ M). Lanes 3-4: contained BSA (15 μ M) and PMA-IB (15 μ M). Lanes 5-6: contained BSA (15 μ M), PMA-IB (15 μ M) and CoHA (1 mM). Lane 7: contained BSA (15 μ M) and CoHA (1 mM). Samples in lanes 2, 3 and 5 were dark controls, while samples in lanes 4, 6 and 7 were irradiated at 346 nm for 10 min.

In addition, the photocleavage of HSA also has been investigated in this study. The results obtained from the study indicated that the fragmentation of HSA by PMA-IB did not occur under the same conditions as in the experiment of BSA (Figure 21).

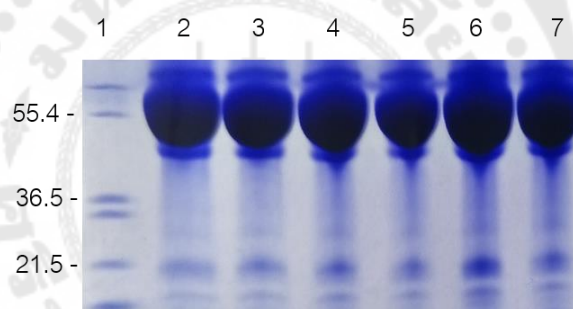


Figure 21 SDS-PAGE of the cleavage reaction of HSA with PMA-IB.

Lane 1: contained protein markers, indicated in kDa. Lane 2: contained BSA (15 μ M). Lanes 3-4: contained BSA (15 μ M) and PMA-IB (15 μ M). Lanes 5-6: contained BSA (15 μ M), PMA-IB (15 μ M) and CoHA (1 mM). Lane 7: contained BSA (15 μ M) and CoHA (1 mM). Samples in lanes 2, 3 and 5 were dark controls, while samples in lanes 4, 6 and 7 were irradiated at 346 nm for 10 min.

1.3 Protein binding studies with PMA-IB

1.3.1 Binding studies

The binding of PMA-IB to proteins has been studied to estimate the photoreagent-protein binding affinity. All absorption spectra of PMA-IB in the absence and presence of protein were recorded using a Shimadzu UV-2401 PC UV-VIS spectrophotometer.

The absorption spectra of the probe in the absence and presence of BSA are shown in Figure 22. When a solution of BSA was added into the PMA-IB solution, blue shifts (5 nm) were observed in the absorption spectra with isosbestic points at 333, 340 and 348 nm. The large blue shifts in the absorption spectra indicated strong binding interaction between the probe and the protein. In addition, the absorption of the spectral changes of PMA-IB in the presence of BSA have been used to analyze the binding constants, which can be obtained from Scatchard equation (discussed in chapter 2). High binding affinity ($9.13 \times 10^5 \text{ M}^{-1}$) was calculated from the linear fit of the plot between r/C_f and r upon binding of PMA-IB to BSA.

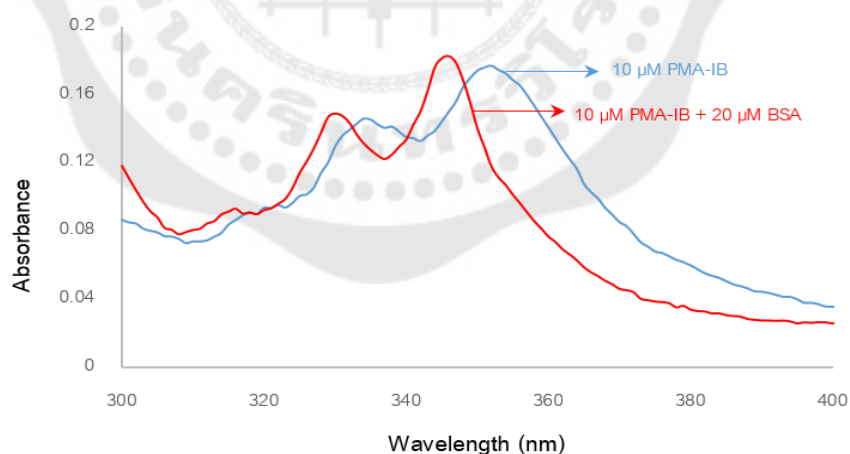


Figure 22 Absorption spectra of PMA-IB in the absence and presence of BSA.

1.3.2 Fluorescence quenching studies

Solvent accessibility of PMA-IB upon binding to the protein was investigated using CoHA as a quencher. All fluorescence spectra of PMA-IB were recorded upon titrating the CoHA into the free PMA-IB and protein-bound PMA-IB.

The fluorescence quenching data were used to estimate the quenching constants (K_{SV}), which can be obtained from the slope of the Stern-Volmer quenching plot (discussed in chapter 2). The Stern-Volmer quenching plot of PMA-IB with CoHA in the absence and presence of BSA is shown in Figure 23. The K_{SV} of BSA-bound PMA-IB was higher than that of free PMA-IB. The increase in the K_{SV} values indicated more accessible of BSA-bound PMA-IB to be quenched by CoHA, suggesting that PMA-IB may bind to BSA at or near surface of the protein, making the orientation of pyrenyl molecule to be more accessible.

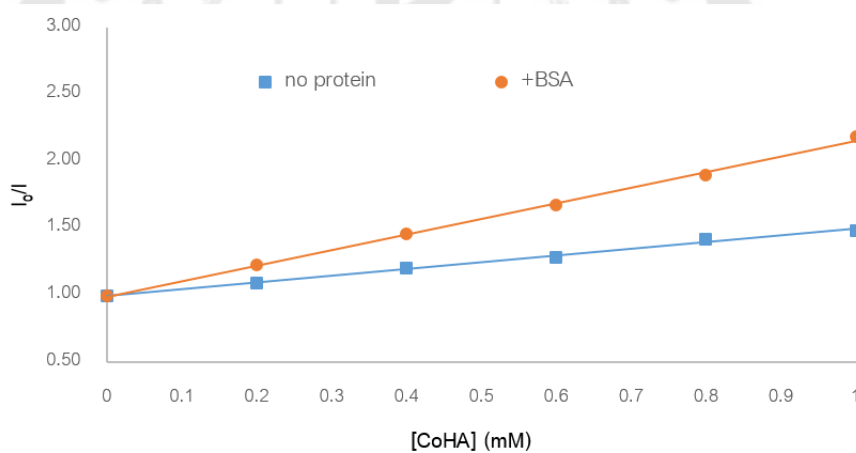


Figure 23 The Stern-Volmer quenching plot of PMA-IB by CoHA in the absence and presence of BSA.

1.4 Molecular docking studies of protein with PMA-IB

To gain a better understanding of how PMA-IB interacts with BSA, molecular docking was applied to examine the interaction in this study. This probe was docked to structure of BSA (PDB ID: 4F5S) using Autodock program (version4.2). The docking results of PMA-IB and BSA are indicated in Figure 24a. Docking studies showed that PMA-IB bound to the subdomain IIIB of BSA with binding free energy of -9.42 kcal/mol. The important amino acid residues interacted with PMA-IB have been indicated in Figure 24b. PMA-IB was found to locate in the close proximity to hydrophobic residues in the subdomain IIIB. Therefore, the interaction between PMA-IB and BSA can possibly be hydrophobic forces.

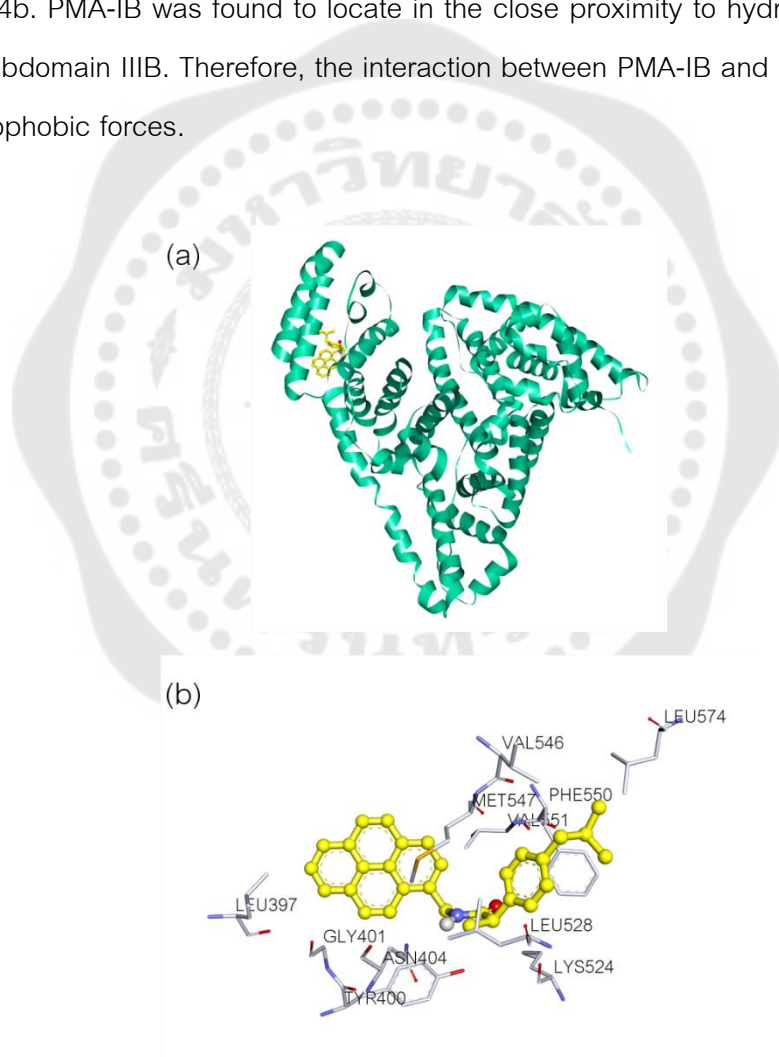


Figure 24 The structure of PMA-IB docked in BSA.

(a) The binding location of PMA-IB upon binding to BSA. (b) The amino acid residues surrounding PMA-IB within 3.5 Å.

The data in the molecular docking studies clearly demonstrated the binding location of PMA-IB upon binding to BSA. These results can support the results obtained from the binding studies and fluorescence quenching studies.



2. Fluorescein derivatives

2.1 Cleavage of protein by fluorescein derivatives

Protein cleaving reaction by fluorescein derivatives has been investigated for the first time in this study. This reaction was successful by activating the reaction mixture of probes, protein and electron acceptor with light at specific wavelength. In this study, Fluorescein sodium salt (F-1), 5(6)-Carboxyfluorescein diacetate (F-2) and Biotin-4-Fluorescein (F-3) (Figure 25) were selected as fluorescent probes to initiate the cleavage reaction of proteins. Lysozyme, avidin, β -lactoglobulin B, concanavalin A, bovine serum albumin (BSA) and human serum albumin (HSA) were chosen as model proteins in this study.

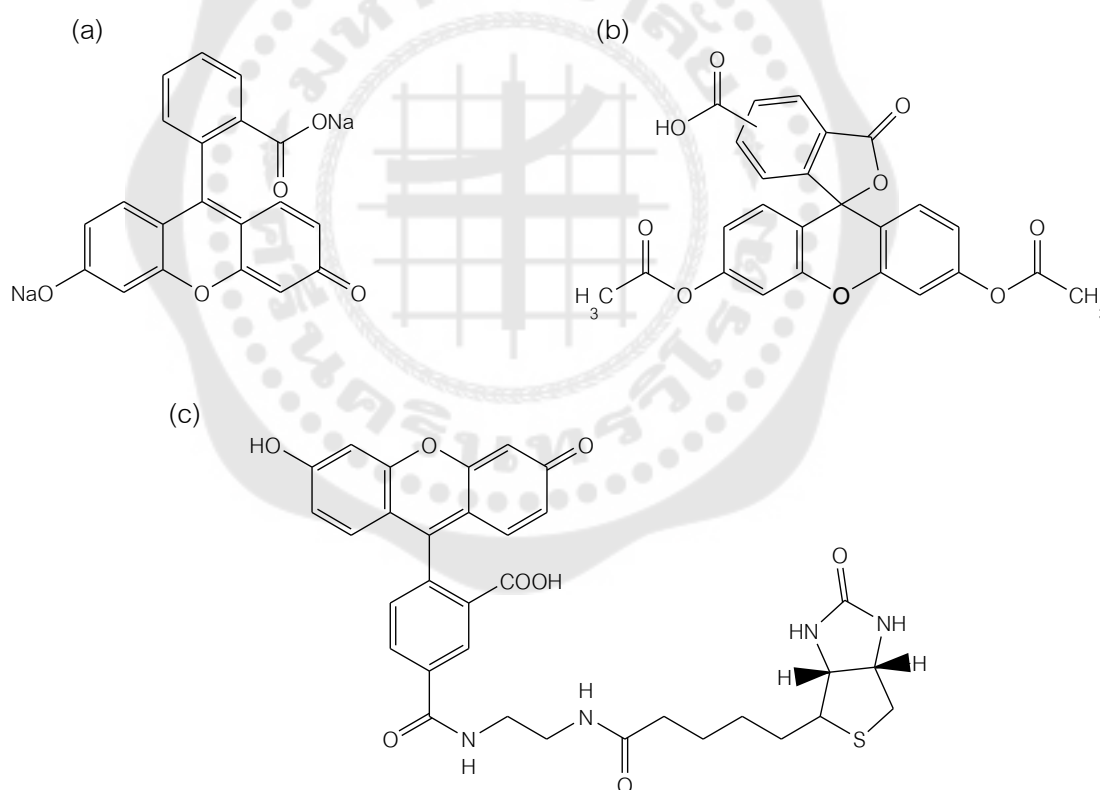


Figure 25 Structures of fluorescein derivatives: (a) Fluorescein sodium salt (F-1), (b) 5(6)-Carboxyfluorescein diacetate (F-2) and (c) Biotin-4-Fluorescein (F-3).

2.1.1 Photocleavage of lysozyme

Photocleavage of lysozyme by fluorescein derivatives was monitored in SDS-PAGE (Figures 26-28). When the solution mixture of lysozyme and fluorescein derivatives was activated with light at specific wavelength (490-494 nm) for 5-20 min, in the presence of CoHA, the new fragments with molecular weights approximately of 10 and 4 kDa were observed on the gel. The molecular weight of these fragments were calculated by comparing the positions of new fragments with the positions of protein markers in the same gel.

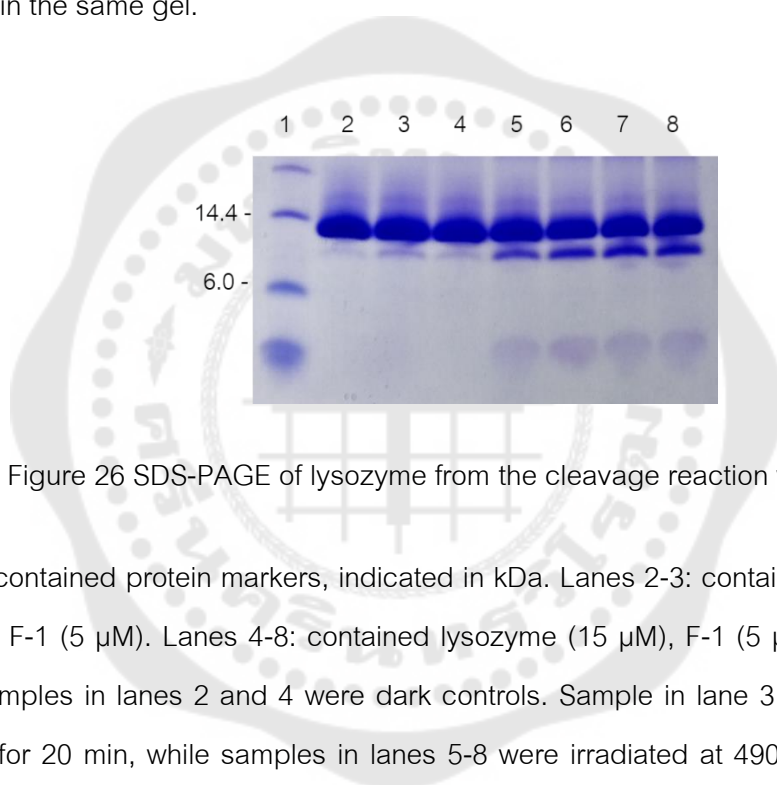


Figure 26 SDS-PAGE of lysozyme from the cleavage reaction with F-1.

Lane 1: contained protein markers, indicated in kDa. Lanes 2-3: contained lysozyme (15 μ M) and F-1 (5 μ M). Lanes 4-8: contained lysozyme (15 μ M), F-1 (5 μ M) and CoHA (1 mM). Samples in lanes 2 and 4 were dark controls. Sample in lane 3 was irradiated at 490 nm for 20 min, while samples in lanes 5-8 were irradiated at 490 nm for 5, 10, 15 and 20 min, respectively.

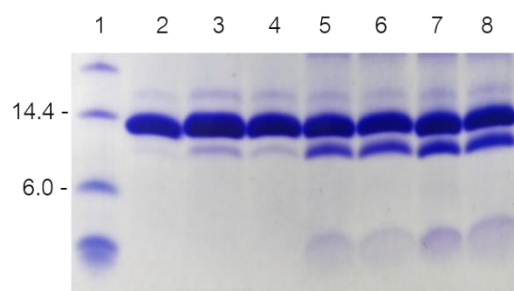


Figure 27 SDS-PAGE of lysozyme from the cleavage reaction with F-2.

Lane 1: contained protein markers, indicated in kDa. Lanes 2-3: contained lysozyme (15 μM) and F-2 (10 μM). Lanes 4-8: contained lysozyme (15 μM), F-2 (10 μM) and CoHA (1 mM). Samples in lanes 2 and 4 were dark controls. Sample in lane 3 was irradiated at 492 nm for 20 min, while samples in lanes 5-8 were irradiated at 492 nm for 5, 10, 15 and 20 min, respectively.

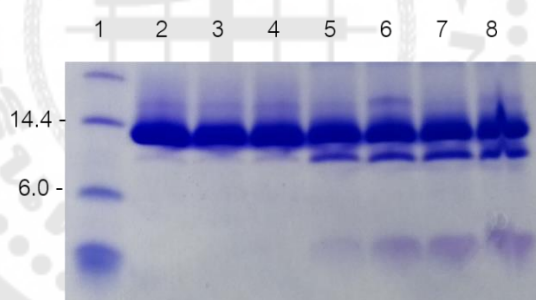


Figure 28 SDS-PAGE of lysozyme from the cleavage reaction with F-3.

Lane 1: contained protein markers, indicated in kDa. Lanes 2-3: contained lysozyme (15 μM) and F-3 (5 μM). Lanes 4-8: contained lysozyme (15 μM), F-3 (5 μM) and CoHA (1 mM). Samples in lanes 2 and 4 were dark controls. Sample in lane 3 was irradiated at 494 nm for 20 min, while samples in lanes 5-8 were irradiated at 494 nm for 5, 10, 15 and 20 min, respectively.

From the photocleavage studies, all three probes (F-1, F-2 and F-3) cleaved lysozyme after exposing the light at specific wavelength for 5 min. The intensity of the new fragment bands increased with increasing of irradiation time. In order to compare the results of protein cleavage properties of all three probes, the cleavage patterns of lysozyme in the presence F-1, F-2 and F-3 were demonstrated in the same gel (Figure 29).

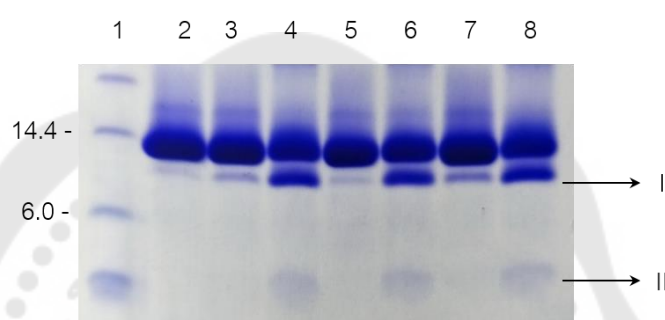


Figure 29 SDS-PAGE of lysozyme from the cleavage reaction with fluorescein derivatives.

Lane 1: contained protein markers, indicated in kDa. Lanes 2-3: contained lysozyme (15 μM), F-1 (10 μM) and CoHA (1 mM). Lanes 4-5: contained lysozyme (15 μM), F-2 (10 μM) and CoHA (1 mM). Lanes 6-7: contained lysozyme (15 μM), F-3 (10 μM) and CoHA (1 mM). Lanes 3, 5 and 7 were irradiated at specific wavelength for 20 min, while samples in lanes 2, 4 and 6 were dark controls.

From Figure 29, two new similar fragments of lysozyme on the gel were observed with all three probes. The yields of the fragment bands obtained from the cleavage of lysozyme were estimated by using ImageJ software (v 1.46r). The cleavage yields of each fragments are demonstrated in Figure 30. The lysozyme cleavage properties of F-1 was found to be the most effective, with highest cleavage yield (43.21%).

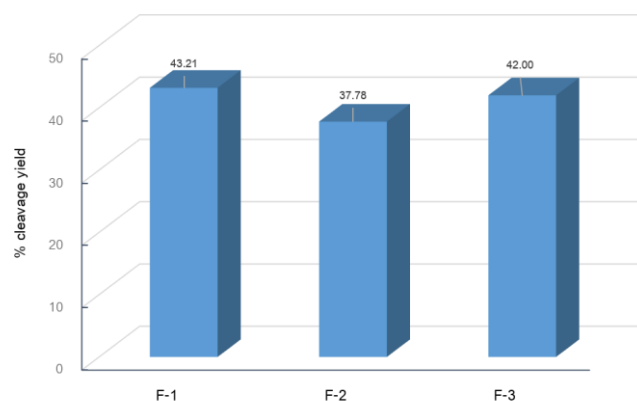


Figure 30 The cleavage yields of peptide fragments from the photoreaction of lysozyme with three fluorescein derivatives.

2.1.2 Photocleavage of avidin

Photocleavage of avidin by F-1, F-2 and F-3 are shown in Figures 31-33. When solution mixture of avidin, fluorescein derivatives and CoHA was exposed the light at specific wavelength (490-494 nm) for 5-20 min, two new fragments with molecular weights approximately of 9 kDa and 5 kDa were found on the gel.

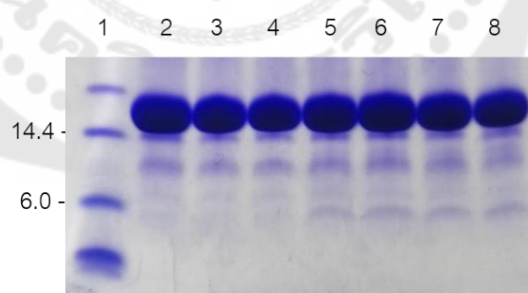


Figure 31 SDS-PAGE of avidin from the cleavage reaction with F-1.

Lane 1: contained protein markers, indicated in kDa. Lanes 2-3: contained avidin (15 μ M) and F-1 (5 μ M). Lanes 4-8: contained avidin (15 μ M), F-1 (5 μ M) and CoHA (1 mM). Samples in lanes 2 and 4 were dark controls. Sample in lane 3 was irradiated at 490 nm for 20 min, while samples in lanes 5-8 were irradiated at 490 nm for 5, 10, 15 and 20 min, respectively.

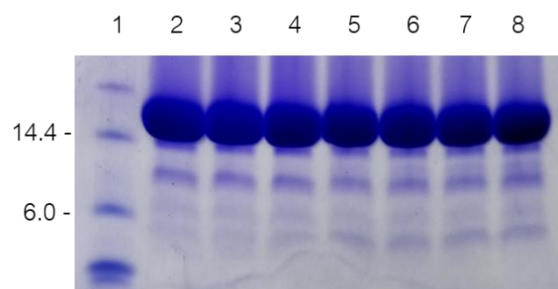


Figure 32 SDS-PAGE of avidin from the cleavage reaction with F-2.

Lane 1: contained protein markers, indicated in kDa. Lanes 2-3: contained avidin (15 μ M) and F-2 (10 μ M). Lanes 4-8: contained avidin (15 μ M), F-2 (10 μ M) and CoHA (1 mM). Samples in lanes 2 and 4 were dark controls. Sample in lane 3 was irradiated at 492 nm for 20 min, while samples in lanes 5-8 were irradiated at 492 nm for 5, 10, 15 and 20 min, respectively.

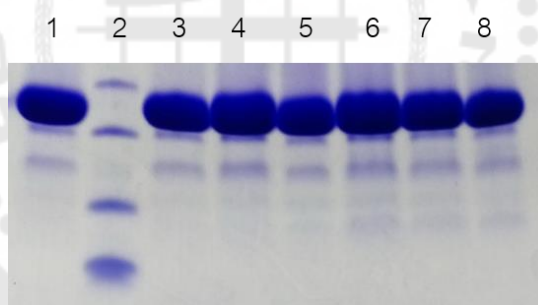


Figure 33 SDS-PAGE of avidin from the cleavage reaction with F-3.

Lane 2: contained protein markers, indicated in kDa. Lanes 1 and 3: contained avidin (15 μ M) and F-3 (5 μ M). Lanes 4-8: contained avidin (15 μ M), F-1 (5 μ M) and CoHA (1 mM). Samples in lanes 1 and 4 were dark controls. Sample in lane 3 was irradiated at 494 nm for 20 min, while samples in lanes 5-8 were irradiated at 494 nm for 5, 10, 15 and 20 min, respectively.

The ability of avidin cleaving reagents was determined by comparing the cleavage yields of avidin with F-1, F-2 and F-3 in the same gel (Figure 34). The cleavage yields are shown in Figure 35. From the studies, F-1 has the most ability to cleave avidin with the highest yield (12.50%).

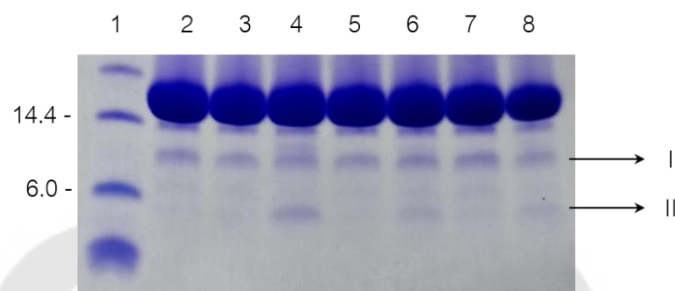


Figure 34 SDS-PAGE of avidin from the cleavage reaction with fluorescein derivatives.

Lane 1: contained protein markers, indicated in kDa. Lanes 2-3: contained avidin (15 μ M), F-1 (10 μ M) and CoHA (1 mM). Lanes 4-5: contained avidin (15 μ M), F-2 (10 μ M) and CoHA (1 mM). Lanes 6-7: contained avidin (15 μ M), F-3 (10 μ M) and CoHA (1 mM). Lanes 3, 5 and 7 were irradiated at specific wavelength for 20 min, while samples in lanes 2, 4 and 6 were dark controls.

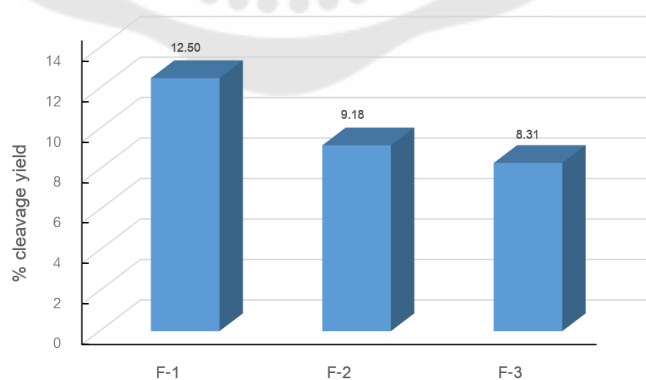


Figure 35 The cleavage yields of peptide fragments from the photoreaction of avidin with fluorescein derivatives.

N-terminal sequencing of the two cleaved fragments (I and II) of avidin from the reactions with F-1 and F-2 showed the same sequences, KFSES and ARKCS, respectively, in which ARKCS was the known N-terminal sequence of avidin (DeLange & Huang, 1971). From the sequencing data, the results indicated that avidin was cleaved between Trp70 – Lys71 (Figure 37). In case of F-3, the cleaved fragments were too faint and unable to be isolated from the gel. Therefore, the N-terminal sequencing analysis of the cleaved fragments of avidin by F-3 cannot be accomplished.

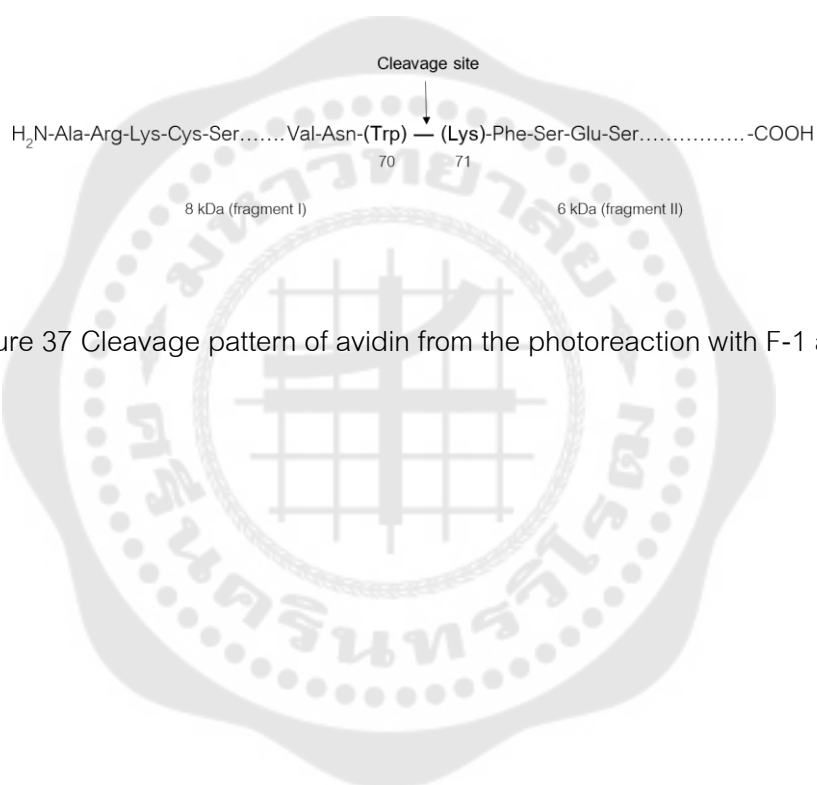


Figure 37 Cleavage pattern of avidin from the photoreaction with F-1 and F-2.

2.3 Protein binding studies with fluorescein derivatives

2.3.1 Binding studies

The absorption titration of fluorescein derivatives by proteins has been studied to estimate the binding affinity of the probes upon binding to the protein. The absorption spectra of F-1, F-2 and F-3 in the absence and presence of lysozyme are shown in Figure 38. In the presence of lysozyme, the absorption peak intensities of all three probes was decreased (hypochromism) by the gradual addition of lysozyme. The small hypochromism of F-1, F-2 and F-3 spectra were calculated for 2.8%, 7.5% and 4.5%, respectively. However, no significant changes of the peak position were observed, indicating that the environment surrounding of these probes in lysozyme could be polar. In addition, the absorbance changes have been used to calculate for the binding constants of fluorescein derivatives bound to lysozyme, which can be obtained from Scatchard equation (discussed in chapter 2). The binding constants of fluorescein derivatives are summarized in Table 1.

Table 1 Binding properties of fluorescein derivatives with lysozyme.

Fluorescein derivatives	K_b (M^{-1})	Hypochromism
F-1	1.47×10^5	2.8 %
F-2	6.31×10^5	7.5 %
F-3	2.42×10^5	4.5 %

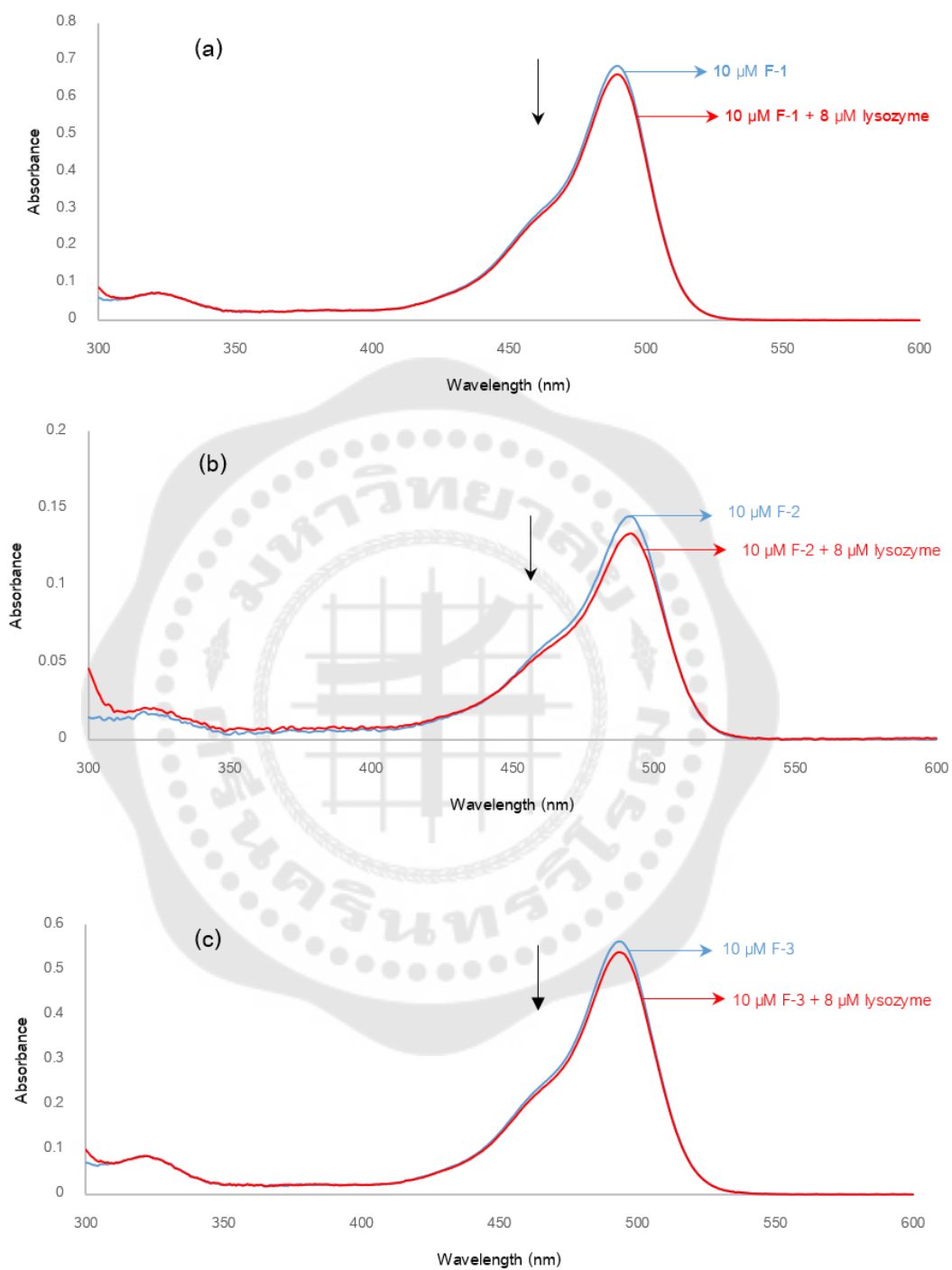


Figure 38 Absorption spectra of (a) F-1, (b) F-2 and (c) F-3 in the absence and presence of lysozyme.

In case of avidin, when titration of three probes with avidin, the absorption spectra of F-2, in the presence of avidin, showed hypochromism of 4.1 %, and no shifts were noted (Figure 39b). In contrast, when titration of F-1 and F-3 with avidin, a small red shift was observed in the absorption spectra as well as hypochromism of 17.4 and 31.7%, respectively (Figures 39a and 39c). Binding constants from the interaction between three probes and avidin are shown in Table 2.

Table 2 Binding properties of fluorescein derivatives with avidin.

Fluorescein derivatives	K_b (M^{-1})	Hypochromism
F-1	6.03×10^5	17.4 %
F-2	1.08×10^5	4.1 %
F-3	7.22×10^5	31.7 %

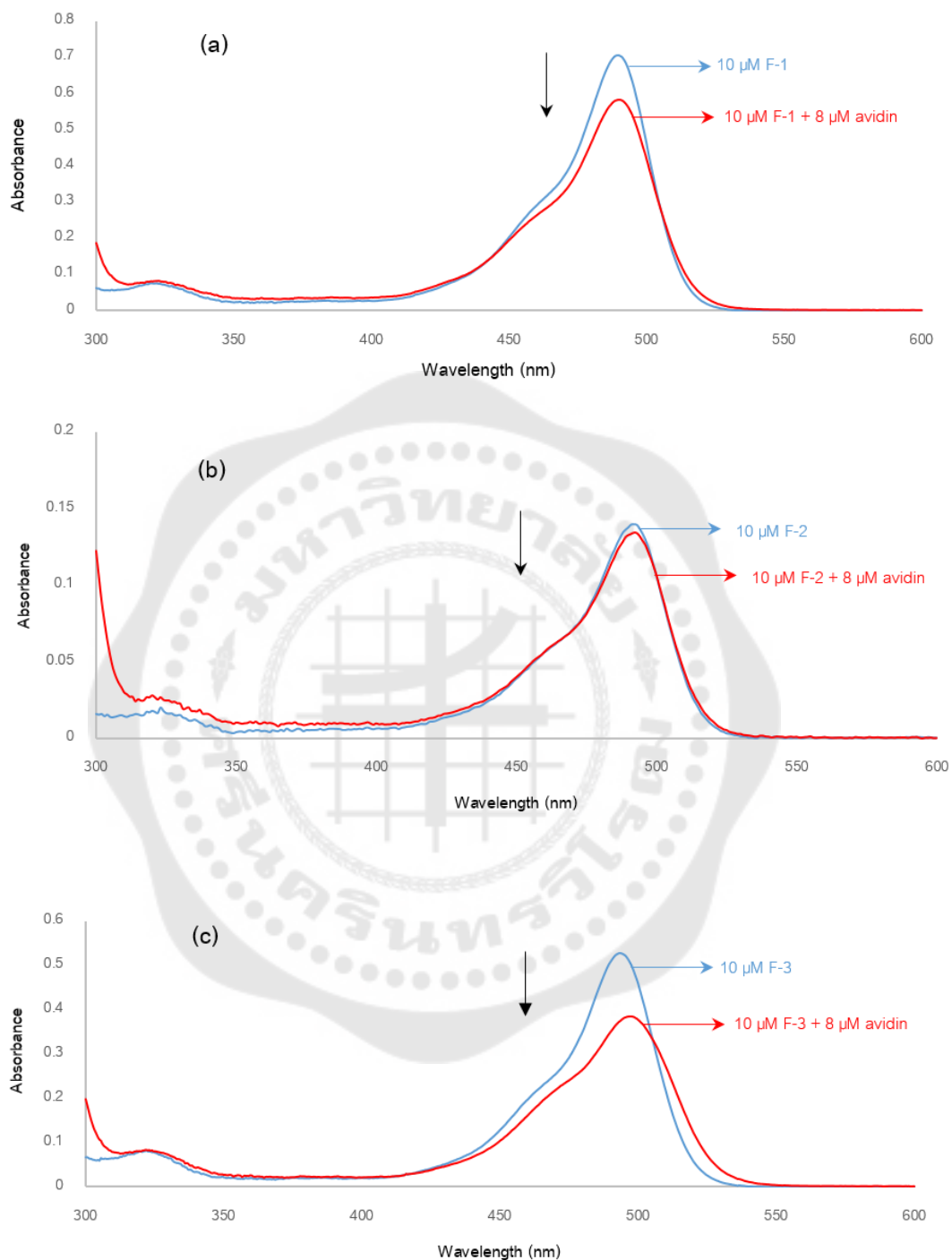


Figure 39 Absorption spectra of (a) F-1, (b) F-2 and (c) F-3 in the absence and presence of avidin.

From the results of binding studies, F-1 and F-3 bound to avidin with higher binding constants than binding to lysozyme. In case of F-2, binding to lysozyme showed higher binding constant than binding to avidin. The distinction of absorbance changes of the probes in the presence of the proteins indicated the differences in the binding location and microenvironment surrounding of these probes upon binding to each protein. Therefore, the side chain in the probe structure has shown an important role on the binding interaction.

2.3.2 Fluorescence quenching studies

The fluorescence quenching of free probes and protein-bound probes by CoHA have been investigated to test the solvent accessibility of the probes while binding to the protein. When titration of free probes and protein-bound F-1, F-2 or F-3 with CoHA (0-1 mM), the quenching constants (K_{sv}) can be calculated from the slope of the Stern-Volmer quenching plot. The K_{sv} values and the Stern-Volmer quenching plots are shown in Table 3 and Figure 40, respectively.

Table 3 The quenching constants (K_{sv}) of fluorescein derivatives with CoHA.

Protein	K_{sv} of F-1, M^{-1}	K_{sv} of F-2, M^{-1}	K_{sv} of F-3, M^{-1}
No protein	1204	1761	1174
Lysozyme	691	808	652
Avidin	238	358	57

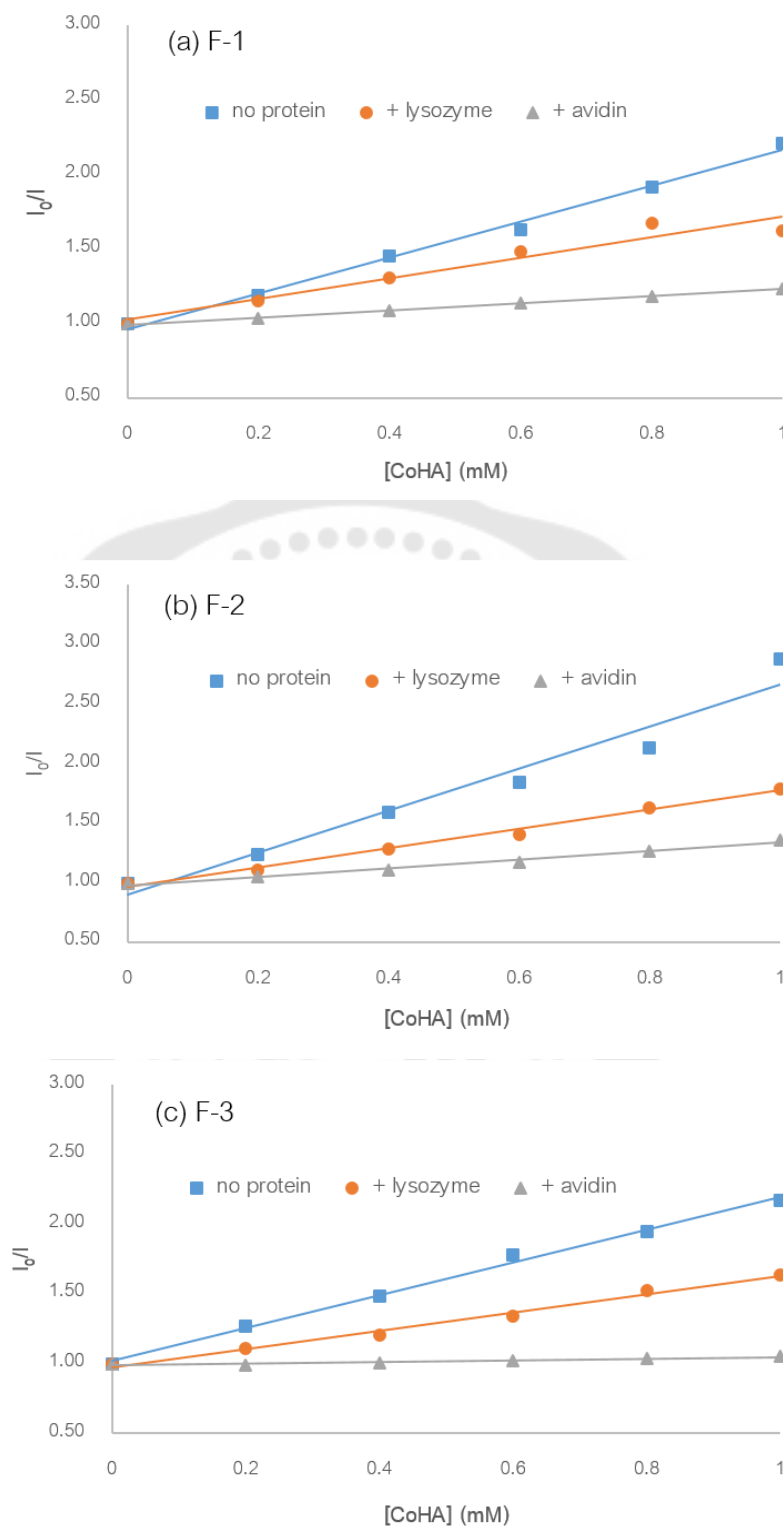


Figure 40 The Stern-Volmer quenching plots of F-1 (a), F-2 (b) and F-3 (c) by titration with CoHA (0-1 mM), in the absence and presence of protein (lysozyme or avidin).

The K_{sv} values of F-1, F-2 and F-3 decreased by 43%, 54% and 44%, respectively, when binding to lysozyme, while the K_{sv} values of F-1, F-2 and F-3 decreased by 80%, 80% and 95%, respectively, when binding to avidin, compared to those of free probes. The decrease in the K_{sv} values indicated the less accessibility of the probes upon binding to the protein. The drastically decreased of K_{sv} values, in case of avidin, suggested that the probes bound in the interior of avidin, which could be protected from the quencher by the protein matrix. In contrast, in case of lysozyme, the decrease of K_{sv} values is less than in case of avidin. These results suggested that the probes bound at or near the surface of lysozyme, which could be less protected from the quencher by protein matrix.

These quenching data correlated with the cleavage yields from the photocleavage experiments, indicating that deeply buried probes in the protein matrix, away from the solvent, could lead to the generation of less reactive intermediates on light excitation, resulting to less cleavage yields.

2.4 Molecular docking studies of protein with F-1, F-2 and F-3

The binding location and binding mode between three probes and proteins, avidin and lysozyme, have been investigated by molecular docking. These probes were docked to the structures of lysozyme (PDB ID: 4XAD) and avidin (PDB ID: 1AVD) using Autodock program (version4.2).

In case of lysozyme, the docking results of F-1 and lysozyme are indicated in Figure 41. Docking studies showed that F-1 was surrounded by 11 amino acid residues (Leu56, Gln57, Ile58, Asn59, Trp62, Trp63, Asn106, Ala107, Trp108, Val109 and Arg112). The hydrogen bonding interaction were observed between the probe and Trp63, Trp108.

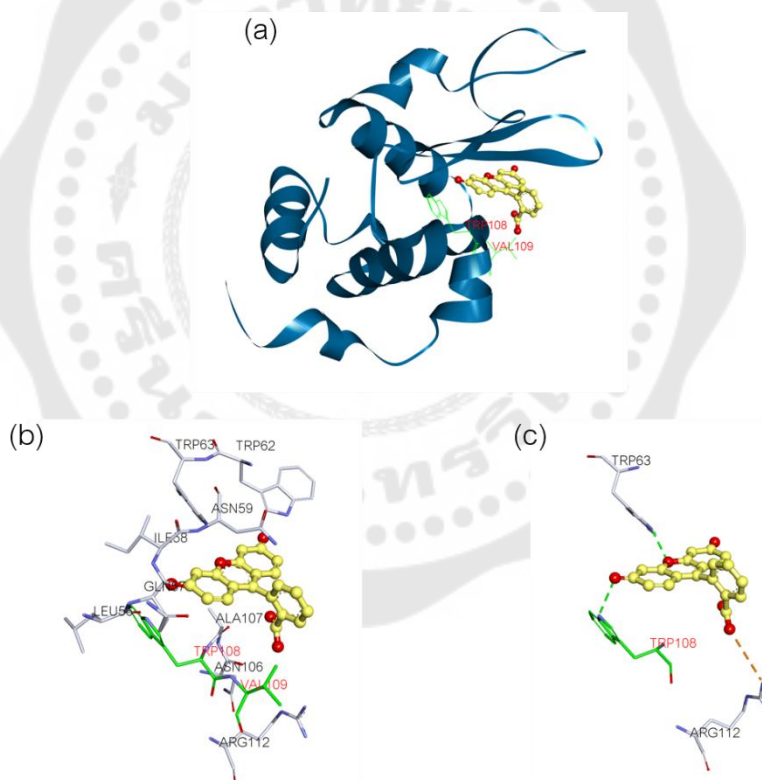


Figure 41 The structure of F-1 docked to lysozyme.

(a) The binding location of F-1 upon binding to lysozyme. (b) The amino acid residues surrounding F-1. (c) The hydrogen bonding (dotted green line) and electrostatic interaction (dotted orange line) between the residues of lysozyme and F-1.

The best docking results between F-2 and lysozyme are indicated in Figure 42. Docking studies showed that F-2 is surrounded by 10 amino acid residues (Asp48, Ile58, Asn59, Arg61, Trp62, Trp63, Ala107, Trp108, Val109 and Arg112). The hydrogen bonding interactions were observed between the probe and Asn59, Arg61, Trp63.

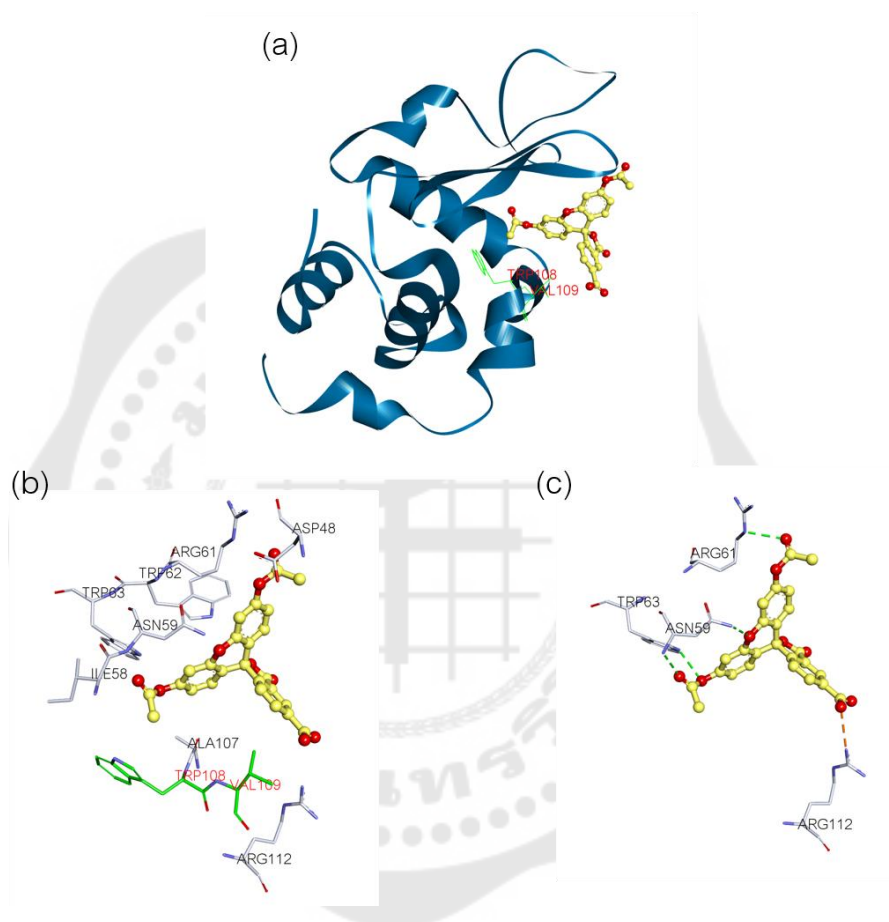


Figure 42 The structure of F-2 docked to lysozyme.

(a) The binding location of F-2 upon binding to lysozyme. (b) The amino acid residues surrounding F-2. (c) The hydrogen bonding (dotted green line) and electrostatic interaction (dotted orange line) between the residues of lysozyme and F-2.

The best docking results between F-3 and lysozyme are indicated in Figure 43. Docking studies showed that F-3 was surrounded by 15 amino acid residues (Glu35, Asn44, Arg45, Asn46, Asp52, Leu56, Gln57, Ile58, Asn59, Trp62, Trp63, Ala107, Trp108, Val109 and Arg112). The hydrogen bonding interactions were observed between the probe and Glu35, Asn46, Asp52, Trp63, Trp108.

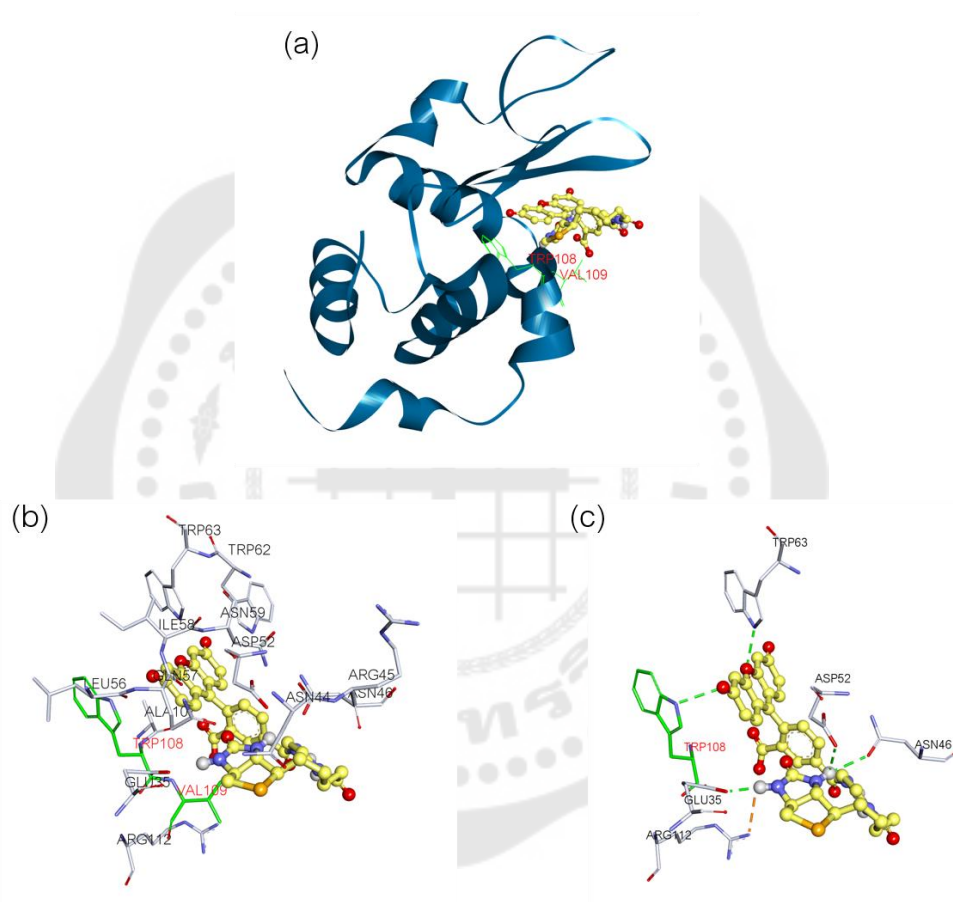


Figure 43 The structure of F-3 docked to lysozyme.

(a) The binding location of F-3 upon binding to lysozyme. (b) The amino acid residues surrounding F-3. (c) The hydrogen bonding (dotted green line) and electrostatic interaction (dotted orange line) between the residues of lysozyme and F-3.

Docking results of the probe upon binding to lysozyme showed that F-1, F-2 and F-3 can bind on the surface of lysozyme, which is correlated to the results from fluorescence quenching studies and protein photocleavage studies. The binding free energy of the most stable F-1, F-2 and F-3 docked to lysozyme were estimated as -8.29, -9.78 and -10.05 kcal/mol, respectively. The binding free energy of F-2 and F-3 were not significantly different, consistent to the binding constant (K_b) obtained from binding studies (Table 4). The small differences of the binding free energy of these probes could result from the different structure size of the probes and the distances from the amino acid residues that interacted with them.

Table 4 Binding constants (K_b) of fluorescein derivatives with lysozyme from binding studies and binding free energies from molecular docking studies.

Photochemical reagent	Binding constant, K_b (M^{-1})	Binding free energy (kcal/mol)
F-1	1.47×10^5	-8.29
F-2	6.31×10^5	-9.78
F-3	2.42×10^5	-10.05

In case of avidin, the docking results of F-1 and avidin are indicated in Figure 44. Docking studies showed that F-1 was surrounded by 15 amino acid residues (Leu14, Ser16, Tyr33, Thr35, Val37, Ala39, Trp70, Lys71, Phe72, Ser73, Thr77, Phe79, Trp97, Leu99 and Asn118). The hydrogen bonding interaction were observed between the probe and Ser73, Thr77.

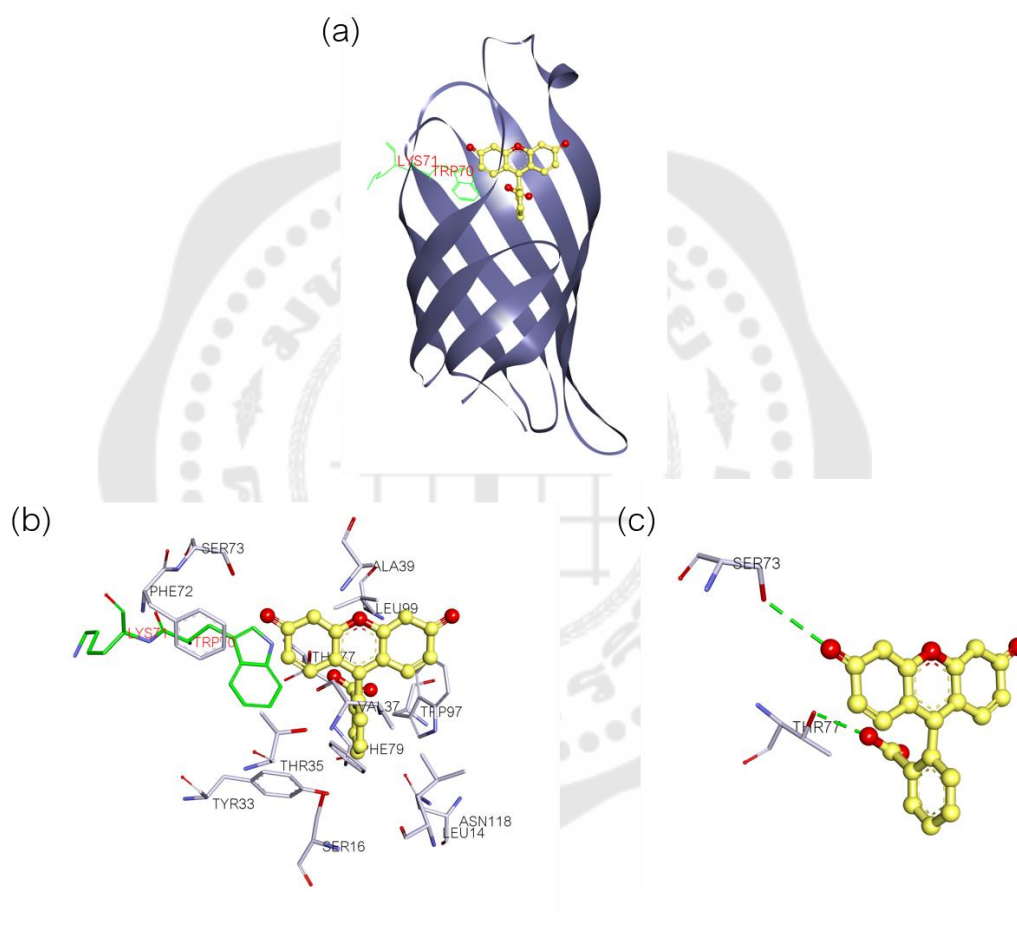


Figure 44 The structure of F-1 docked to avidin.

(a) The binding location of F-1 upon binding to avidin. (b) The amino acid residues surrounding F-1. (c) The hydrogen bonding between the residues of avidin and F-1 (dotted green line).

The best docking results from the binding interaction between F-2 and avidin are indicated in Figure 45. Docking studies showed that F-2 was surrounded by 13 amino acid residues (Asp13, Leu14, Thr35, Val37, Thr38, Trp70, Lys71, Phe72, Trp97, Arg114, Gly116, Ile117 and Asn118). The hydrogen bonding interactions were observed between the probe and Arg114, Ile117.

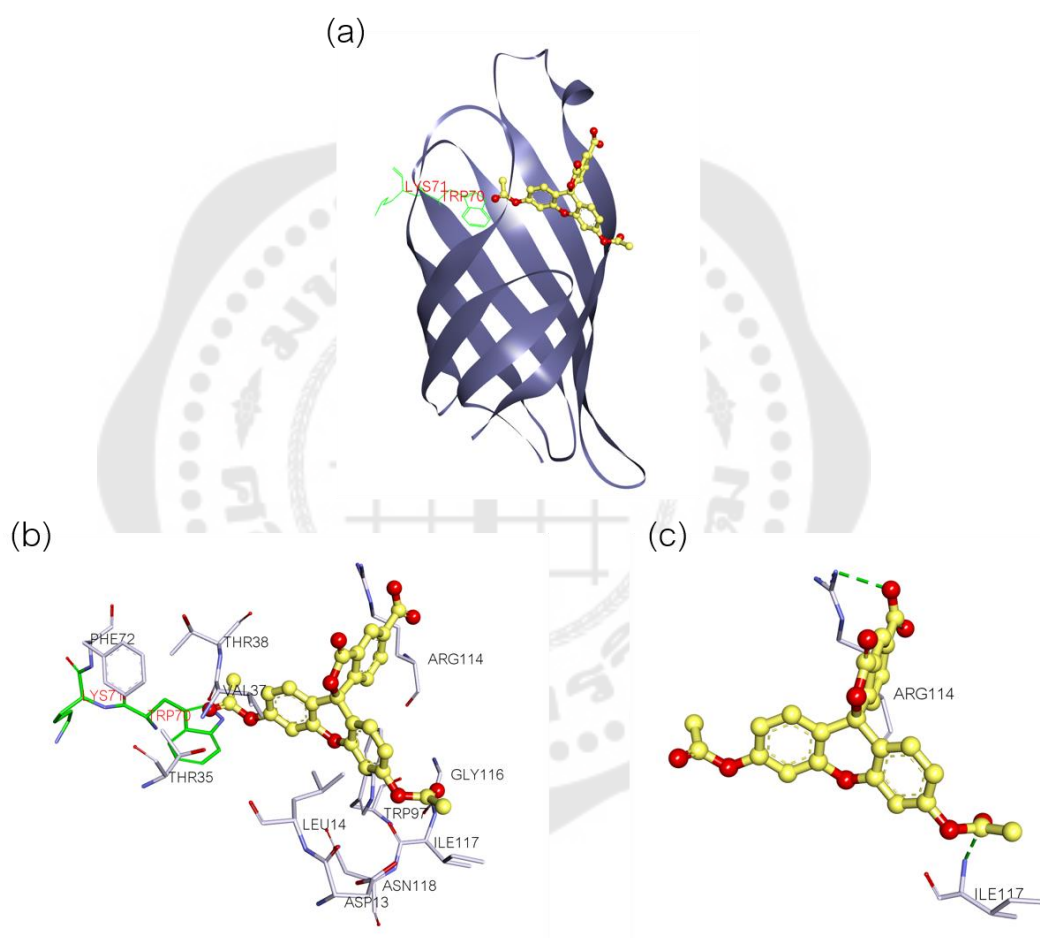


Figure 45 The structure of F-2 docked to avidin.

(a) The binding location of F-2 upon binding to avidin. (b) The amino acid residues surrounding F-2. (c) The hydrogen bonding between the residues of avidin and F-2 (dotted green line).

The best docking results obtained from the binding interaction between F-3 and avidin are indicated in Figure 46. Docking studies showed that F-3 was surrounded by 18 amino acid residues (Asn12, Asp13, Leu14, Ser16, Tyr33, Thr35, Val37, Thr38, Ala39, Trp70, Lys71, Ser73, Trp97, Leu99, Arg114, Gly116, Ile117 and Asn118). The hydrogen bonding interactions were observed between the probe and Asn12, Asp13, Ser16, Tyr33, Ser73, Arg114, Ile117, Asn118.

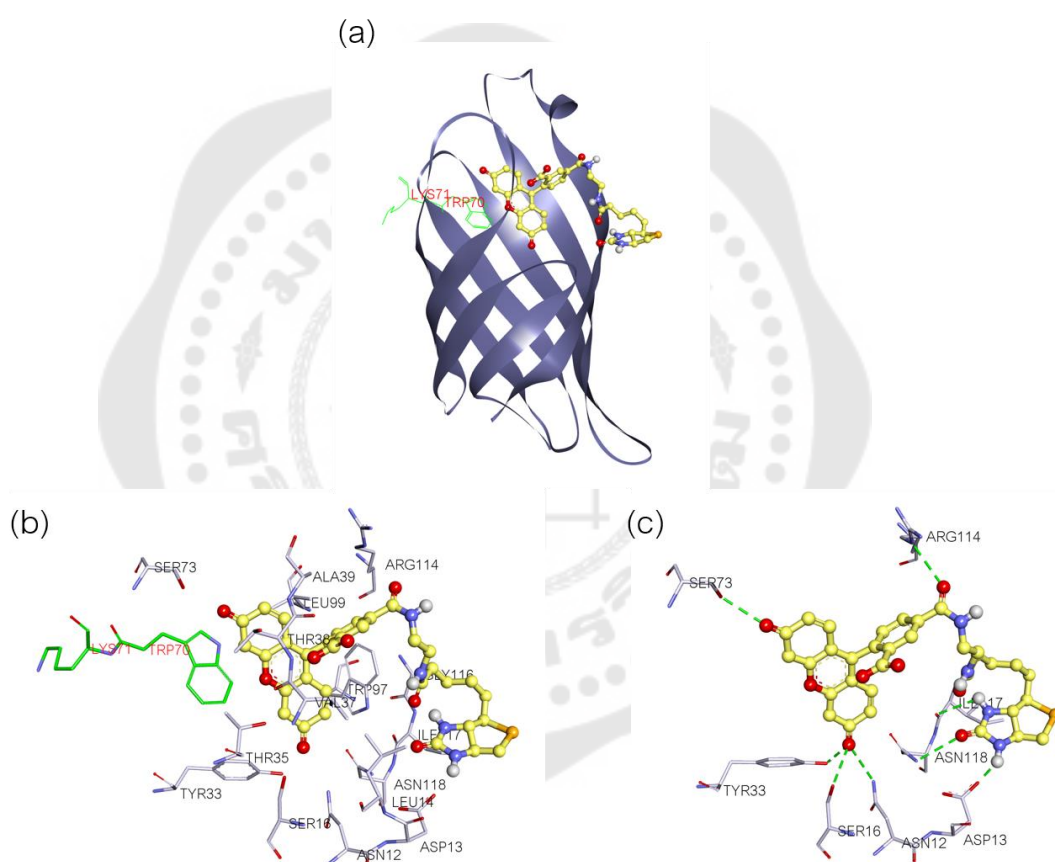


Figure 46 The structure of F-3 docked to avidin.

(a) The binding location of F-3 upon binding to avidin. (b) The amino acid residues surrounding F-3. (c) The hydrogen bonding between the residues of avidin and F-3 (dotted green line).

From the docking results of avidin, F-1, F-2 and F-3 were bound to avidin with binding free energy of -9.46, -8.20 and -10.57 kcal/mol, respectively. The binding free energies of these probes indicated that the binding interaction of F-3 with avidin was the most stable, which was related to the binding constant (K_b) obtained from the binding studies (Table 5). In addition, the docking results supported the cleavage experiments in which the cleavage site occurred between Trp70 – Lys71 from the reaction with F-1 and F-2.

Table 5 Binding constants (K_b) of fluorescein derivatives with avidin from binding studies and binding free energies from molecular docking studies.

Photochemical reagent	Binding constant, K_b (M^{-1})	Binding free energy (kcal/mol)
F-1	6.03×10^5	-9.46
F-2	1.08×10^5	-8.20
F-3	7.22×10^5	-10.57

The data in the molecular docking studies clearly demonstrated the binding location and binding affinity of three probes upon binding to lysozyme and avidin. These results can support the results obtained from the binding studies, fluorescence quenching studies and protein photocleavage studies.

3. Metal complex

The use of molybdenum (VI) peroxy α -amino acid complexes for cleavage of pepsin under photo and thermal conditions have been recently reported (Jityuti et al., 2015; Jityuti et al., 2013). The results in these researches indicated the important role of the amino acid side chain attaching to the molybdenum complexes for binding to pepsin at specific region. Therefore, in this study, the ability of $\text{MoO}(\text{O}_2)_2(\text{asparagine})(\text{H}_2\text{O})$ to cleave pepsin was investigated to gain more understanding of the effect of amino acid side chain in the molybdenum complex on the binding and cleavage reactions.

3.1 Synthesis of $\text{MoO}(\text{O}_2)_2(\text{asparagine})(\text{H}_2\text{O})$: Mo-asn

Mo-asn was synthesized by dissolving molybdenum trioxide (MoO_3) in hydrogen peroxide. Asparagine was added to the above solution mixture, resulting in the yellow crystal product (yield: 72.36 %).

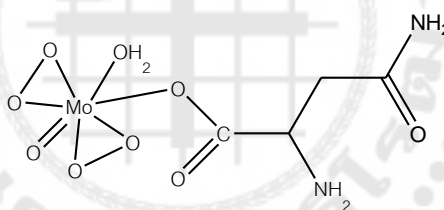


Figure 47 Structure of $\text{MoO}(\text{O}_2)_2(\text{asparagine})(\text{H}_2\text{O})$: Mo-asn.

3.2 Photocleavage of pepsin by molybdenum complex

In photocleavage reaction, molybdenum complex can cleave pepsin at specific site upon activation by light. In this study, photocleavage of pepsin by Mo-asn was monitored in SDS-PAGE (Figure 48). When the solution mixture of pepsin and Mo-asn was irradiated with light at 320 nm and 340 nm for 10-30 min, the new fragments with molecular weights approximately of 22 and 9 kDa were observed on the gel.

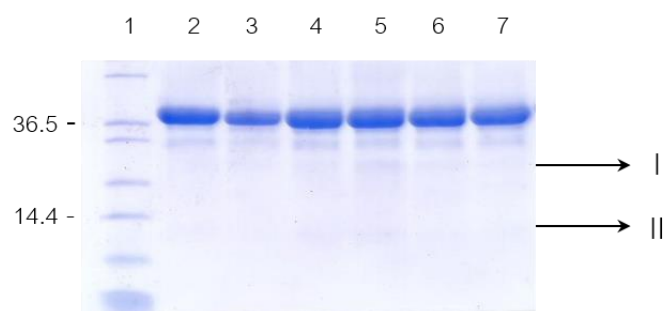


Figure 48 SDS-PAGE of pepsin from the cleavage reaction with Mo-asn.

Lane 1: contained protein markers, indicated in kDa. Lanes 2-7: contained pepsin (15 μ M) and Mo-asn (2 mM). Sample in lane 2 was dark control. Samples in lanes 3-5 were irradiated at 320 nm for 10, 20 and 30 min, respectively, while samples in lanes 6-7 were irradiated at 340 nm for 10 and 20 min, respectively.

From SDS-PAGE, the photocleavage of pepsin by Mo-asn was observed when irradiating pepsin-probe mixture with light at 320 nm and 340 nm for 10 min (lanes 4 and 6, respectively). Increasing the irradiation time from 10 to 30 min increased the cleavage yield of reaction (Figure 49). The highest cleavage yield of pepsin (5.55%) was obtained when using the light at 320 nm for 30 min. However, the cleavage of pepsin irradiated at 340 nm for 10 and 20 min gave faint bands of the cleaved fragments (lanes 6-7, respectively). The results corresponded to the absorbance of Mo-asn, in which the amount of light absorbed at 320 nm was greater than that at 340 nm. This made the cleavage yield from the reaction at 320 nm to be higher than the cleavage yield obtained from the reaction at 340 nm.

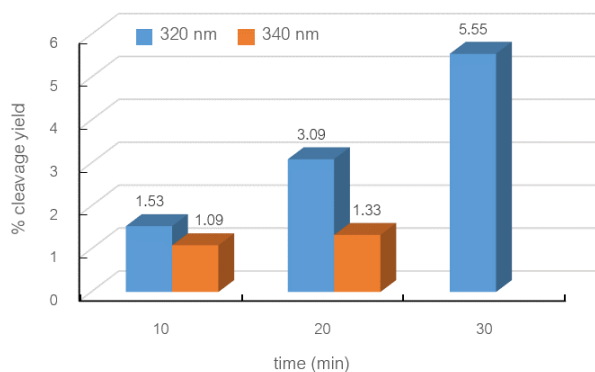


Figure 49 The cleavage yields of peptide fragments from the photoreaction of pepsin with Mo-asn.

3.3 Thermal cleavage of pepsin by molybdenum complex

In thermal cleavage reaction, metal complexes have been developed to probe specific binding sites on proteins and subsequent activation with heat to cleave protein *via* oxidative or hydrolytic reactions. In oxidative reaction, cleavage of protein was successful by incubation the reaction mixture of metal complex and protein with reducing agent and H_2O_2 (which generated the hydroxyl radical for initiation of the protein cleavage reaction). In case of hydrolytic reaction, protein cleavage reaction was achieved without the requirement of a reducing agent and H_2O_2 . Therefore, the reaction pathway (oxidation or hydrolysis) of thermal cleavage of pepsin by molybdenum complex was investigated in this study. In addition, the conditions of this reaction (concentration of Mo-asn and incubation time) were also optimized in this experiment.

The thermal cleavage reaction of pepsin by Mo-asn was investigated by incubation the solution mixture of Mo-asn (1 mM) and pepsin (15 μ M) at 37 °C for 24 h. The progress of the protein cleavage was observed in SDS-polyacrylamide gel electrophoresis experiment (SDS-PAGE), as shown in Figure 50.

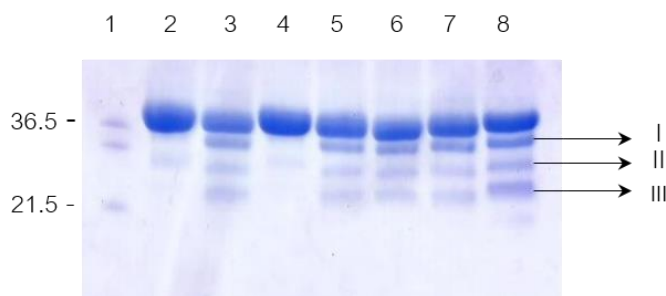


Figure 50 SDS-PAGE of pepsin from the thermal reaction with Mo-asn.

Lane 1: contained protein markers, indicated in kDa. Lane 2: contained pepsin (15 μM). Lane 3: contained pepsin (15 μM) and Mo-asn (1 mM). Lanes 4-5: contained pepsin (15 μM), Mo-asn (1 mM), H_2O_2 (1mM) and ASC (1 mM). Lane 6: contained pepsin (15 μM), Mo-asn (1 mM), and ASC (1 mM). Lane 7: contained pepsin (15 μM), Mo-asn (1 mM) and H_2O_2 (1mM). Lane 8: contained pepsin (15 μM), H_2O_2 (1mM) and ASC (1 mM). Samples in lanes 2 and 4 were heat controls. Samples in lanes 3, 5, 6, 7 and 8 were incubated at 37 $^\circ\text{C}$ for 24 h.

From SDS-PAGE, pepsin was cleaved by Mo-asn in the absence and presence of ascorbic acid and H_2O_2 (lanes 3 and lane 5, respectively), resulting to three new observed fragments with molecular weights approximately of 30, 26 and 22 kDa. However, the addition of reducing agent and H_2O_2 to the reaction may damage the side chains of protein and the resulting cleaved peptide fragments cannot be investigated for the amino acid sequence. Therefore, this study has selected the hydrolytic pathway for the thermal cleavage reaction of pepsin, in which the reducing agent and H_2O_2 were not needed.

The thermal cleavage reaction of pepsin with various concentrations of Mo-asn was investigated in this study. The solution mixtures of pepsin (15 μM) and various concentrations of Mo-asn were incubated at 37 $^\circ\text{C}$ for 24 h. The results in this study were monitored in SDS-PAGE, as shown in Figure 51.

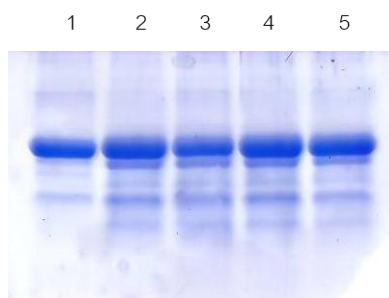


Figure 51 SDS-PAGE of pepsin from the thermal reaction with Mo-asn.

Lanes 1: contained pepsin (15 μ M) and Mo-asn (1.000 mM). Lanes 2-5: contained pepsin (15 μ M) and Mo-asn at concentrations of 1.000, 0.500, 0.250, 0.125 mM, respectively. Sample in lane 1 was heat control. Samples in lanes 2-5 were incubated at 37 $^{\circ}$ C for 24 h.

From SDS-PAGE, thermal cleavage of pepsin by Mo-asn was successful when incubation of pepsin with Mo-asn 0.125 mM (lane 5). Increasing the concentration of molybdenum complex from 0.125 to 1.000 mM increased the cleavage yield (Figure 52). The highest cleavage yield of pepsin (19.80%) was obtained when incubation of pepsin with 1.000 mM Mo-asn.

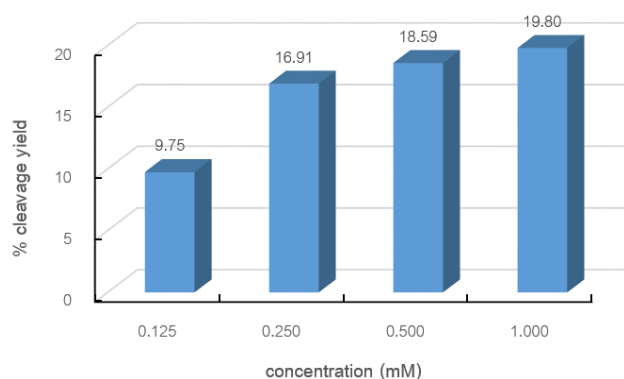


Figure 52 The cleavage yields of peptide fragments from the thermal reaction of pepsin with Mo-asn.

The thermal cleavage of pepsin by Mo-asn also depended on the incubation time. When incubation of pepsin (15 μ M) and Mo-asn (1 mM) at 37 $^{\circ}$ C for 2-24 h, the progress of the protein cleavage was observed on gel as shown in Figure 53.

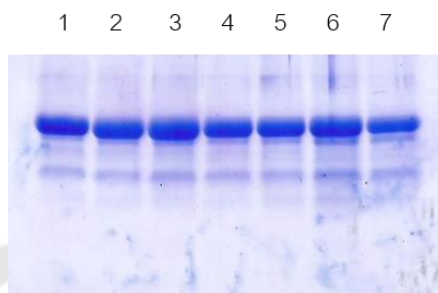


Figure 53 SDS-PAGE of pepsin from the cleavage reaction with Mo-asn.

Lanes 1-7: contained pepsin (15 μ M) and Mo-asn (1 mM). Sample in lanes 1 was heat control while samples in lanes 2-7 were incubated at 37 $^{\circ}$ C for 2, 4, 6, 12, 20, 24 h, respectively.

From SDS-PAGE, pepsin was cleaved by Mo-asn when incubation of the pepsin with Mo-asn for 2 h (lane 2). The cleavage yields of new fragment bands were increased with increasing time of incubation (Figure 54). Incubation of pepsin with Mo-asn for 24 h, resulted in the highest cleavage yield (14.83%).

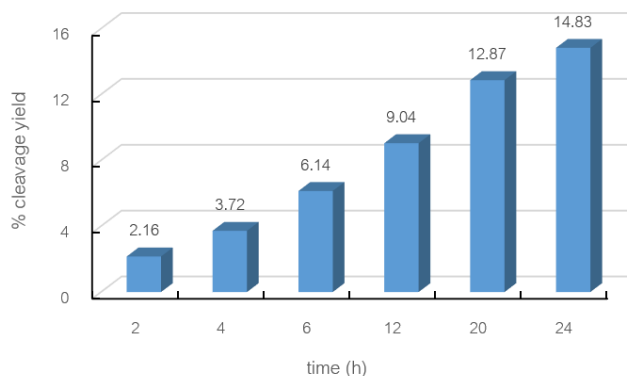


Figure 54 The cleavage yields of peptide fragments by thermal reaction of pepsin and Mo-asn.

In addition, the other model proteins such as lysozyme, avidin, β -lactoglobulin B, concanavalin A, BSA and HSA were chosen to investigate the thermal cleavage reaction with Mo-asn in this study. The results obtained from these studies indicated that Mo-asn did not cleave these proteins under the same conditions with pepsin (data not shown).

CHAPTER 5

CONCLUSION AND DISCUSSION

The main objective in this research was to investigate the ability of chemical reagents to initiate the cleavage of proteins at specific site. These probes can serve as potential artificial peptidases for creating smaller fragments that are more amenable for amino acid sequencing. In addition, such probes can also contribute to the fundamental understanding of the interaction between probes and proteins. A major class of protein cleaving reagents in this study included of: (1) pyrene derivative, (2) fluorescein derivatives, and (3) metal complex.

1. Pyrene derivative

The selective cleavage of proteins by new pyrene derivative (PMA-IB) has been investigated by binding the probe to the target site on protein and subsequent irradiation with light at maximum absorption wavelength of the probe to cleave the protein backbone. In this study, photocleavage of BSA by PMA-IB was successful by irradiating the solution mixture of BSA, PMA-IB and electron acceptor, cobalt (III) hexamine trichloride (CoHA) at 346 nm for 10 min. The cleavage of BSA resulted in two new cleaved fragments with molecular weights approximately of 45 and 22 kDa. Binding studies, fluorescence quenching studies and molecular docking were used to examine the binding location and binding affinity of this probe on protein. The data in these studies clearly demonstrated the binding properties of PMA-IB upon binding to BSA, in which PMA-IB bound to protein with high affinity ($9.13 \times 10^5 \text{ M}^{-1}$) and PMA-IB was located within the subdomain IIIB of BSA. The amino acid residues surrounding this probe within 3.5 Å consisted of Leu397, Try400, Asn404, Lys524, Leu528, Val546, Met547, Phe550, Val551 and Leu574. When considering the binding site of PMA-IB with the two new fragments from the cleavage experiment (molecular weights of 45 and 22 kDa), the cleavage site of BSA may occur at position between Leu397– Gly398 (Figure 55). In addition, current results demonstrated that the photocleavage of protein did not occur in the absence of PMA-IB, CoHA or light. Therefore, the mechanism of this

reaction may occur from the formation of reactive intermediates, which is resulted from quenching of the excited probe by CoHA. These reactive intermediates can be expected to play the important role in the photocleavage reaction. However, the detailed understanding of the mechanism for cleavage of protein needs more examinations.

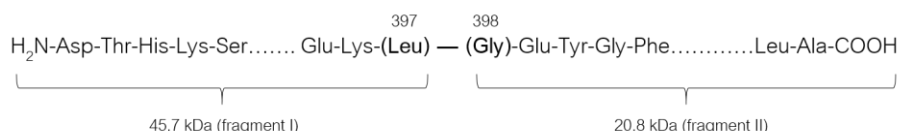


Figure 55 Cleavage pattern of BSA from photoreaction with PMA-IB.

2. Fluorescein derivatives

Although, the pyrene derivatives were used as a protein cleaving reagent in many researches, but the solubility of pyrene derivatives has a limit in aqueous solution. Therefore, the use of fluorescein derivatives as fluorescent probes for initiation the protein cleavage reaction was designed in this study. These probes are highly soluble in aqueous solution and give strong absorption band in visible region. Here, the efficacy of fluorescein derivatives to cleave proteins backbone is reported for the first time. All three probes (F-1, F-2 and F-3) cleaved lysozyme and avidin after exposure the light at specific wavelength (490-494 nm), in the presence of CoHA. Lysozyme was cleaved by three probes resulting in at least two fragments with molecular weights approximately of 10 and 4 kDa. N-terminal amino acid sequencing of peptide fragments indicated cleavage site between Trp108 and Val109 of lysozyme by all three probes. In order to compare the cleavage yield of three probes, F-1 was found to be the most effective for cleavage of lysozyme, with highest cleavage yield (43.21%).

To understand the interaction between all three probes and lysozyme, binding studies, fluorescence quenching studies and molecular docking were applied to examine the interaction between the probe and protein. The results of these studies clarified the binding location and binding affinity of F-1, F-2 and F-3 on lysozyme, which corresponded to the results obtained from the protein photocleavage studies.

In case of avidin, two cleaved fragments with molecular weights approximately of 9 kDa and 5 kDa were observed on the gel. N-terminal amino acid sequencing of cleaved fragments indicated the same cleavage site of avidin by F-1 and F-2 at between Trp70 – Lys71. However, the cleavage site of avidin by F-3 could not be achieved. When comparing the cleavage yield of F-3 with the yield of F-1 and F-2, F-3 indicated the lowest cleavage yield (8.31%). Therefore, the new cleaved fragments from the gel were unable to be isolated and analyzed for amino acid sequencing. However, the cleavage site of avidin when activated with F-3 can be predicted by considering with the results obtained from the photocleavage experiment and molecular docking. The data of these studies indicated that the cleavage site of avidin may occur at position between Trp70 – Lys71.

3. Metal complex

From the ability of three molybdenum (VI) peroxo α -amino acid complexes, $\text{MoO}(\text{O}_2)_2(\alpha\text{-leucine})(\text{H}_2\text{O})$, $\text{MoO}(\text{O}_2)_2(\alpha\text{-glutamine})(\text{H}_2\text{O})$ and $\text{MoO}(\text{O}_2)_2(\alpha\text{-glycine})(\text{H}_2\text{O})$, cleaved of pepsin at different cleavage sites (Jityuti et al., 2015; Jityuti et al., 2013). These results indicated that the selectivity of the probe on protein depended on the charges and the lengths of the amino acid side chains attaching to molybdenum. Therefore, current experiment was designed to examine the effect of amino acid side chain of molybdenum complex on the cleavage properties. Asparagine was chosen as amino acid residue for attaching to molybdenum. The side chain of asparagine and glutamine contained NH_2 at the end, but the lengths are different. Thus, the ability of the Mo-asn on pepsin has been investigated, and pepsin was successfully cleaved by activating the solution mixture of Mo-asn and pepsin with light and heat. The cleaved pepsin resulted in at least two fragments with molecular weights approximately of 22 and 9 kDa under photo condition, and resulted to at least three fragments with molecular weights approximately of 30, 26 and 22 kDa under thermal condition. The cleavage site of pepsin when activated with Mo-asn can be predicted by considering the molecular weight of new fragments with the molecular structure of pepsin (from Protein Data bank, PDB ID: 1YX9). From the results, the cleavage site of pepsin may occur at positions

REFERENCES

- Abou-Zied, O. K., & Sulaiman, S. A. J. (2014). Site-specific recognition of fluorescein by human serum albumin: A steady-state and time-resolved spectroscopic study. *Dyes and Pigments*, *110*, 89-96.
- Barbero, N., Barni, E., Barolo, C., Quagliotto, P., Viscardi, G., Napione, L., . . . Bussolino, F. (2009). A study of the interaction between fluorescein sodium salt and bovine serum albumin by steady-state fluorescence. *Dyes Pigments*, *80*(3), 307-313.
- Bio-Rad. (2017). Mini Trans-Blot® Electrophoretic Transfer Cell Retrieved from www.bio-rad.com/webroot/web/pdf/lsr/literature/M1703930.pdf
- Boyer, R. (2002). *Concepts in biochemistry*. Pacific Grove, CA: Brooks/Cole Thomson Learning.
- Brew, K., Vanaman, T. C., & Hill, R. L. (1967). Comparison of the amino acid sequence of bovine alpha-lactalbumin and hens egg white lysozyme. *J. Biol. Chem.*, *242*, 3747-3749.
- Buranaprapuk, A., & Kumar, C. V. (2018). Jedi's light sabre: site specific photocleavage of proteins with light. *SWU Sci. J.*, *34*, 1-17.
- Buranaprapuk, A., Kumar, C. V., Jockusch, S., & Turro, N. J. (2000). Photochemical protein scissors: Role of aromatic residues on the binding affinity and photocleavage efficiency of pyrenyl peptides. *Tetrahedron*, *56*, 7019-7025.
- Buranaprapuk, A., Malaikaew, Y., Svasti, J., & Kumar, C. V. (2008). Chiral protein scissors activated by light: Recognition and protein photocleavage by a new pyrenyl probe. *J Phys Chem B*, *112*, 9258-9265.
- D'Alessandro, M. L., Ellis, D. A., Carter, J. A., Stock, N. L., & March, R. E. (2013). Competitive binding of aqueous perfluorooctanesulfonic acid and ibuprofen with bovine serum albumin studied by electrospray ionization mass spectrometry. *Int J Mass Spectrom*, *345-347*, 28-36.
- DeLange, R. J., & Huang, T. S. (1971). Egg white avidin, 3. Sequence of the 78-residue middle cyanogen bromide peptide. Complete amino acid sequence of the protein

- subuni. *J. Biol. Chem.*, 246, 698-709.
- Djordjevic, C., Vuletic, N., Jacobs, B. A., Renslo, M. L., & Sinn, E. (1997). Molybdenum(VI) peroxo α -amino acid complexes: Synthesis, spectra, and properties of $\text{MoO}(\text{O}_2)_2(\alpha\text{-aa})(\text{H}_2\text{O})$ for $\alpha\text{-aa}$ = glycine, alanine, proline, valine, leucine, serine, asparagine, glutamine, and glutamic acid. X-ray crystal structures of the glycine, alanine, and proline compounds. *Inorg Chem*, 36, 1798-1805.
- Elokely, K. M., & Doerksen, R. J. (2013). Docking challenge: protein sampling and molecular docking performance. *J Chem Inf Model*, 53(8), 1934-1945.
- Gerald, K., Heinz, F., & Hermann, J. G. (1999). Accurate measurement of avidin and streptavidin in crude biofluids with a new, optimized biotin-fluorescein conjugate. *Biochim Biophys Acta*, 1427, 33-43.
- Gerald, K., Karl, K., Heinz, F., & Hermann, J. G. (1999). Rapid estimation of avidin and streptavidin by fluorescence quenching or fluorescence polarization. *Biochim Biophys Acta*, 1427, 44-48.
- Ghaim, J. B., Greiner, D. P., Meares, C. F., & Gennis, R. B. (1995). Proximity mapping the surface of a membrane protein using an artificial protease. *Biochemistry*, 34, 11311-11315.
- Hoyer, D., Cho, H., & Schultz, P. G. (1990). A new strategy for selective protein cleavage. *J Am Chem Soc*, 112, 3249-3250.
- Jasinska, A., Ferguson, A., Mohamed, W. S., & Szreder, T. (2009). The study of interactions between ibuprofen and bovine serum albumin. *Scientific Bulletin of the Technical University of Lodz, Food Chemistry and Biotechnology*, 73, 15-24.
- Jityuti, B., Buranaprapuk, A., & Liworncharoenpong, T. (2015). Artificial metallopeptidases: Protein cleavage by molybdenum(VI) peroxo α -amino acid complexes. *Inorg Chem Commun*, 55, 129-131.
- Jityuti, B., Liworncharoenpong, T., & Buranaprapuk, A. (2013). Use of a molybdenum(VI) complex as artificial protease in protein photocleavage. *J Photochem Photobiol B*, 126, 55-59.
- Jyotsna, T., Kumar, C. V., Jockusch, S., & Turro, N. J. (2010). Steady-state and time-

- resolved studies of the photocleavage of lysozyme by Co(III) complexes. *Langmuir*, 26(3), 1966-1972.
- Kahne, D. C., & Skill, W. C. (1988). Hydrolysis of peptide bond in neutral water. *J. Am. Chem. Soc.*, 110, 7529-7534.
- Kumar, C. V., & Buranaprapuk, A. (1997). Site-specific photocleavage of proteins. *Angew Chem Int Ed Engl*, 36, 2085-2087.
- Kumar, C. V., & Buranaprapuk, A. (1999). Tuning the selectivity of protein photocleavage: Spectroscopic and photochemical studies. *J Am Chem SOC*, 121, 4262-4270.
- Kumar, C. V., Buranaprapuk, A., Cho, A., & Chaudhari, A. (2000). Artificial metallopeptidases: regioselective cleavage of lysozyme. *Chem Commun*(7), 597-598.
- Kumar, C. V., Buranaprapuk, A., Opiteck, G. J., Moyer, M. B., Jockusch, S., & Turro, N. J. (1998). Photochemical protease: Site-specific photocleavage of hen egg lysozyme and bovine serum albumin. *Proc Natl Acad Sci*, 95, 10361-10366.
- Kumar, C. V., Buranaprapuk, A., Sze, H. O., Jockusch, S., & Turro, N. J. (2002). Chiral protein scissors: High enantiomeric selectivity for binding and its effect on protein photocleavage efficiency and specificity. *Proc Natl Acad Sci*, 99, 5810-5815.
- Kumar, C. V., Buranaprapuk, A., & Thota, J. (2002). Protein scissors: Photocleavage of proteins at specific locations. *Proc Indian Acad. Sci*, 114, 579-592.
- Kumar, C. V., & Thota, J. (2005). Photocleavage of lysozyme by cobalt(III) complexes. *Inorg Chem*, 44, 825-827.
- Li, J., & Yao, P. (2009). Self-assembly of ibuprofen and bovine serum albumin-dextran conjugates leading to effective loading of the drug. *Langmuir*, 25, 6385-6391.
- Malaikaew, P., Svasti, J., Kumar, C. V., & Buranaprapuk, A. (2011). Photocleavage of avidin by a new pyrenyl probe. *J Photochem Photobiol B*, 103(3), 251-255.
- Moran, L. A., Horton, R. A., Scrimgeour, G., & Perry, M. (2014). *Principles of biochemistry*. Harlow: Pearson Education Limited.
- Nelson, D. L., & Cox, M. M. (2008). *Lehninger principles of biochemistry*. New York: W. H. Freeman and company.

- Ninfa, A. J., & Ballou, D. P. (1998). *Fundamental laboratory approaches for biochemistry and biotechnology*. Bethesda, MD: Fitzgerald Science Press, Inc.
- Rana, T. M., & Meares, C. F. (1991). Iron chelate mediated proteolysis: protein structure dependence. *J. Am. Chem. Soc.*, *113*, 1859-1861.
- Rub, M. A., Khan, J. M., Asiri, A. M., Khan, R. H., & ud-Din, K. (2014). Study on the interaction between amphiphilic drug and bovine serum albumin: A thermodynamic and spectroscopic description. *J Lumin*, *155*, 39-46.
- Scatchard, G. (1949). The attractions of proteins for small molecules and ions. *Ann. N. Y. Acad. Sci.*, *51*, 660-672.
- Schagger, H., & Jagow, G. V. (1987). Tricine - sodium dodecyl sulfate - polyacrylamide gel electro-phoresis for the separation of proteins in the range from 1 to 100 kDa. *Anal Biochem*, *166*, 368-379.
- Shahabadi, N., Khorshidi, A., & Moghadam, N. H. (2013). Study on the interaction of the epilepsy drug, zonisamide with human serum albumin (HSA) by spectroscopic and molecular docking techniques. *Spectrochim Acta A Mol Biomol Spectrosc*, *114*, 627-632.
- Stern, O., & Volmer, M. (1919). über die Abklingzeit der Fluoreszenz *Phys. Z.*, *20*, 183-188.
- Sulaiman, S. A. J., Kulathunga, H. U., & Abou-Zied, O. K. (2015). Spectroscopic characterization of the binding mechanism of fluorescein and carboxyfluorescein in human serum albumin. *Proc of SPIE*, *9339*, 9339081-9339010.
- Voet, D., Voet, J. G., & Pratt, C. W. (2013). *Principles of biochemistry*. Hoboken, NJ: John Wiley & Sons, Inc.
- Yadav, R., Das, S., & Sen, P. (2012). Static and Dynamic Aspects of Supramolecular Interactions of Coumarin 153 and Fluorescein with Bovine Serum Albumin. *Aust J Chem*, *65*(9), 1305-1313.
- Yamasaki, K., Chuang, V. T., Maruyama, T., & Otagiri, M. (2013). Albumin-drug interaction and its clinical implication. *Biochim Biophys Acta*, *1830*(12), 5435-5443.
- Zhang, Q., Ni, Y., & Kokot, S. (2010). Molecular spectroscopic studies on the interaction between ractopamine and bovine serum albumin. *J Pharm Biomed Anal*, *52*(2),

280-288.

Zheng, M., Liu, X., Xu, Y., Li, H., Luo, C., & Jiang, H. (2013). Computational methods for drug design and discovery: focus on China. *Trends Pharmacol Sci*, 34(10), 549-559.





APPENDIX

APPENDIX

SDS-PAGE of the cleavage reaction of β -lactoglobulin B, concanavalin A, BSA and HSA with fluorescein derivatives have been demonstrated in Figure 57-68.

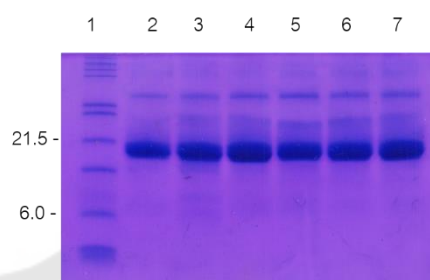


Figure 57 SDS-PAGE of β -lactoglobulin B from the cleavage reaction with F-1.

Lane 1: contained protein markers, indicated in kDa. Lanes 2-3: contained protein (15 μ M) and F-1 (5 μ M). Lanes 4-7: contained protein (15 μ M), F-1 (5 μ M) and CoHA (1 mM). Samples in lanes 2 and 4 were dark controls. Sample in lane 3 was irradiated at 490 nm for 20 min, while samples in lanes 5-7 were irradiated at 490 nm for 10, 20 and 30 min, respectively.

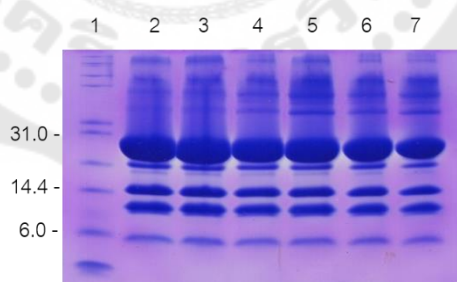


Figure 58 SDS-PAGE of concanavalin A from the cleavage reaction with F-1.

Lane 1: contained protein markers, indicated in kDa. Lanes 2-3: contained protein (15 μ M) and F-1 (5 μ M). Lanes 4-7: contained protein (15 μ M), F-1 (5 μ M) and CoHA (1 mM). Samples in lanes 2 and 4 were dark controls. Sample in lane 3 was irradiated at 490 nm for 20 min, while samples in lanes 5-7 were irradiated at 490 nm for 10, 20 and 30 min, respectively.

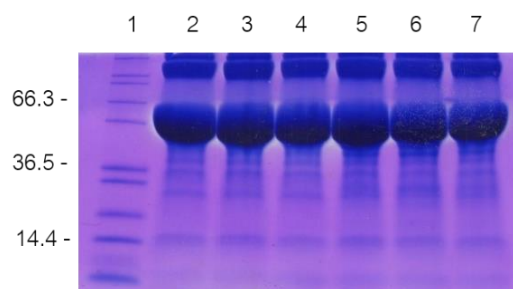


Figure 59 SDS-PAGE of BSA from the cleavage reaction with F-1.

Lane 1: contained protein markers, indicated in kDa. Lanes 2-3: contained protein (15 μ M) and F-1 (5 μ M). Lanes 4-7: contained protein (15 μ M), F-1 (5 μ M) and CoHA (1 mM). Samples in lanes 2 and 4 were dark controls. Sample in lane 3 was irradiated at 490 nm for 20 min, while samples in lanes 5-7 were irradiated at 490 nm for 10, 20 and 30 min, respectively.

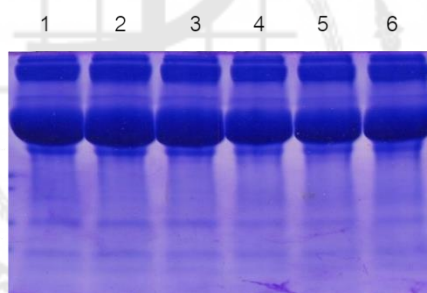


Figure 60 SDS-PAGE of HSA from the cleavage reaction with F-1.

Lanes 1-2: contained protein (15 μ M) and F-1 (5 μ M). Lanes 3-6: contained protein (15 μ M), F-1 (5 μ M) and CoHA (1 mM). Samples in lanes 1 and 3 were dark controls. Sample in lane 2 was irradiated at 490 nm for 20 min, while samples in lanes 4-6 were irradiated at 490 nm for 10, 20 and 30 min, respectively.

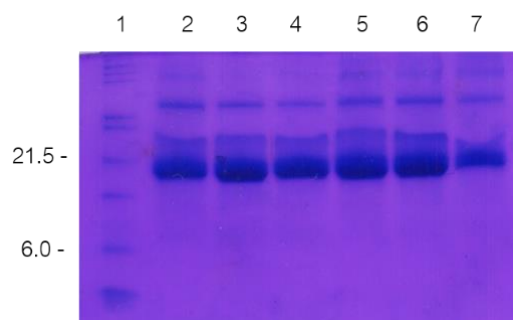


Figure 61 SDS-PAGE of β -lactoglobulin B from the cleavage reaction with F-2.

Lane 1: contained protein markers, indicated in kDa. Lanes 2-3: contained protein (15 μ M) and F-2 (10 μ M). Lanes 4-7: contained protein (15 μ M), F-2 (10 μ M) and CoHA (1 mM). Samples in lanes 2 and 4 were dark controls. Sample in lane 3 was irradiated at 492 nm for 20 min, while samples in lanes 5-7 were irradiated at 492 nm for 10, 20 and 30 min, respectively.

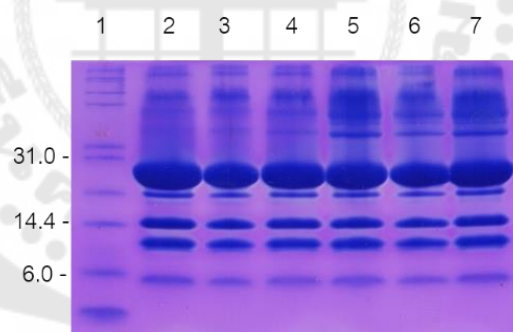


Figure 62 SDS-PAGE of concanavalin A from the cleavage reaction with F-2.

Lane 1: contained protein markers, indicated in kDa. Lanes 2-3: contained protein (15 μ M) and F-2 (10 μ M). Lanes 4-7: contained protein (15 μ M), F-2 (10 μ M) and CoHA (1 mM). Samples in lanes 2 and 4 were dark controls. Sample in lane 3 was irradiated at 492 nm for 20 min, while samples in lanes 5-7 were irradiated at 492 nm for 10, 20 and 30 min, respectively.

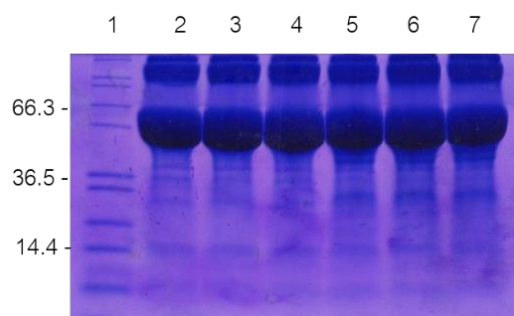


Figure 63 SDS-PAGE of BSA from the cleavage reaction with F-2.

Lane 1: contained protein markers, indicated in kDa. Lanes 2-3: contained protein (15 μ M) and F-2 (10 μ M). Lanes 4-7: contained protein (15 μ M), F-2 (10 μ M) and CoHA (1 mM). Samples in lanes 2 and 4 were dark controls. Sample in lane 3 was irradiated at 492 nm for 20 min, while samples in lanes 5-7 were irradiated at 492 nm for 10, 20 and 30 min, respectively.

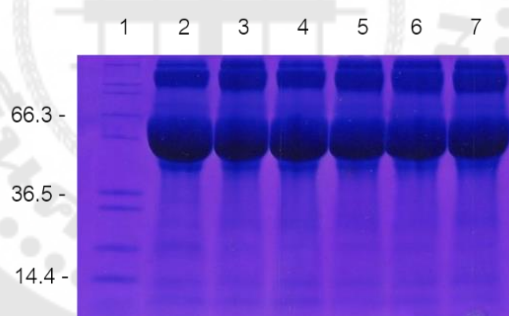


Figure 64 SDS-PAGE of HSA from the cleavage reaction with F-2.

Lane 1: contained protein markers, indicated in kDa. Lanes 2-3: contained protein (15 μ M) and F-2 (10 μ M). Lanes 4-7: contained protein (15 μ M), F-2 (10 μ M) and CoHA (1 mM). Samples in lanes 2 and 4 were dark controls. Sample in lane 3 was irradiated at 492 nm for 20 min, while samples in lanes 5-7 were irradiated at 492 nm for 10, 20 and 30 min, respectively.

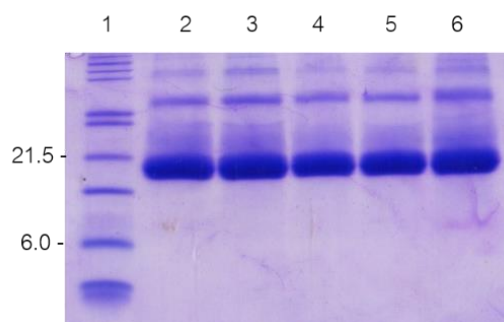


Figure 65 SDS-PAGE of β -lactoglobulin B from the cleavage reaction with F-3.

Lane 1: contained protein markers, indicated in kDa. Lane 2: contained protein (15 μ M) and F-3 (5 μ M). Lanes 3-6: contained protein (15 μ M), F-3 (5 μ M) and CoHA (1 mM). Samples in lanes 2 and 3 were dark controls. Sample in lanes 4-6 were irradiated at 494 nm for 10, 20 and 30 min, respectively.

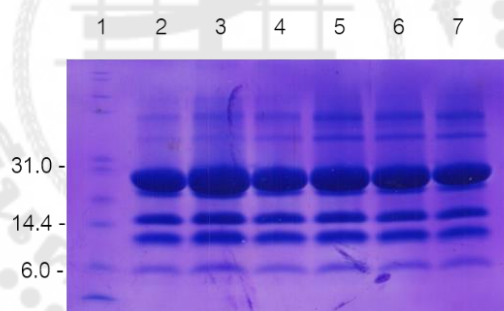


Figure 66 SDS-PAGE of concanavalin A from the cleavage reaction with F-3.

Lane 1: contained protein markers, indicated in kDa. Lanes 2-3: contained protein (15 μ M) and F-3 (5 μ M). Lanes 4-7: contained protein (15 μ M), F-3 (5 μ M) and CoHA (1 mM). Samples in lanes 2 and 4 were dark controls. Sample in lane 3 was irradiated at 494 nm for 20 min, while samples in lanes 5-7 were irradiated at 494 nm for 10, 20 and 30 min, respectively.

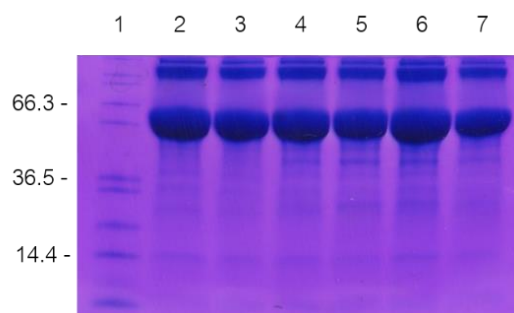


Figure 67 SDS-PAGE of BSA from the cleavage reaction with F-3.

Lane 1: contained protein markers, indicated in kDa. Lanes 2-3: contained protein (15 μ M) and F-3 (5 μ M). Lanes 4-7: contained protein (15 μ M), F-3 (5 μ M) and CoHA (1 mM). Samples in lanes 2 and 4 were dark controls. Sample in lane 3 was irradiated at 494 nm for 20 min, while samples in lanes 5-7 were irradiated at 494 nm for 10, 20 and 30 min, respectively.

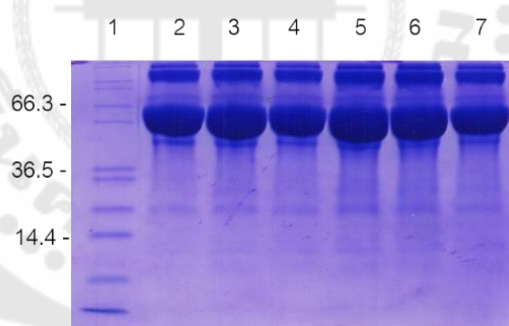


Figure 68 SDS-PAGE of HSA from the cleavage reaction with F-3.

Lane 1: contained protein markers, indicated in kDa. Lanes 2-3: contained protein (15 μ M) and F-3 (5 μ M). Lanes 4-7: contained protein (15 μ M), F-3 (5 μ M) and CoHA (1 mM). Samples in lanes 2 and 4 were dark controls. Sample in lane 3 was irradiated at 494 nm for 20 min, while samples in lanes 5-7 were irradiated at 494 nm for 10, 20 and 30 min, respectively.

VITA

NAME Benchawan Jityuti

DATE OF BIRTH 14 April 1988

PLACE OF BIRTH Angthong

INSTITUTIONS ATTENDED 2010 Bachelor of Science Program in Chemistry
From Srinakharinwirot University

2013 Master of Science Program in Chemistry
From Srinakharinwirot University

2019 Doctor of Philosophy Program in Applied Chemistry
From Srinakharinwirot University

HOME ADDRESS 1 Village No.5, Bang Chao Cha, Phothong, Angthong 14120

